processes

Generation Mechanism of Hydroxyl Free Radicals in Micro–Nanobubbles Water and Its Prospect in Drinking Water

Tianzhi Wang [1,*], Ci Yang [1], Peizhe Sun [1], Mingna Wang [2], Fawei Lin [1], Manuel Fiallos [1] and Soon-Thiam Khu [1,3]

1   School of Environmental Science & Engineering, Tianjin University, Tianjin 300350, China; yc3259672120@163.com (C.Y.); sunpeizhe@tju.edu.cn (P.S.); linfawei@tju.edu.cn (F.L.); manuelfiallos20@gmail.com (M.F.); soon.thiam.khu@tju.edu.cn (S.-T.K.)
2   School of Civil Engineering, Tianjin University, Tianjin 300072, China; mingna.wang@tju.edu.cn
3   Engineering Research Center of City Intelligence and Digital Governance, Ministry of Education of the People's Republic of China, Tianjin 300350, China
*   Correspondence: wangtianzhi@tju.edu.cn

Abstract: Micro–nanobubbles (MNBs) can generate ·OH in situ, which provides a new idea for the safe and efficient removal of pollutants in water supply systems. However, due to the difficulty in obtaining stable MNBs, the generation efficiency of ·OH is low, and the removal efficiency of pollutants cannot be guaranteed. This paper reviews the application research of MNB technology in water security from three aspects: the generation process of MNBs in water, the generation rule of ·OH during MNB collapse, and the control mechanisms of MNBs on pollutants and biofilms. We found that MNB generation methods are divided into chemical and mechanical (about 10 kinds) categories, and the instability of the bubble size restricts the application of MNB technology. The generation of ·OH by MNBs is affected by the pH, gas source, bubble size, temperature, and external stimulation. And the pH and external stimulus have more influence on ·OH generation in situ than the other factors. Adjusting the pH to alkaline or acidic conditions and selecting ozone or oxygen as the gas source can promote ·OH generation. MNB collapse also releases a large amount of energy, during which the temperature and pressure can reach 3000 K and 5 Gpa, respectively, making it efficient to remove ≈90% of pollutants (i.e., trichloroethylene, benzene, and chlorobenzene). The biofilm can also be removed by physical, chemical, and thermal effects. MNB technology also has great application potential in drinking water, which can be applied to improve water quality, optimize household water purifiers, and enhance the taste of bottled water. Under the premise of safety, after letting people of different ages taste water samples, we found that compared with ordinary drinking water, 85.7% of people think MNB water is softer, and 73.3% of people think MNB water is sweeter. This further proves that MNB water has a great prospect in drinking water applications. This review provides innovative theoretical support for solving the problem of drinking water safety.

Keywords: micro–nanobubbles; hydroxyl radical; drinking water security; pollutants; biofilm; engineering application

1. Introduction

Water is the source of life. Eight billion people in the world need to consume about 1.1375×10^{13} m³ of freshwater resources every year, of which drinking water accounts for about 7.3×10^9 m³ [1]. Therefore, ensuring the safety and quality of drinking water is a notable prerequisite to the healthy survival of human society [1]. In recent years, due to population growth and urban expansion, the pollution and shrinkage of water sources and the deterioration of urban water supply network systems have significantly grown, inducing severe water supply system quality issues. Based on this, the existence of emerging and refractory pollutants can create challenges in drinking water safety.

The challenges of drinking water safety mainly focus on water quality changes caused by the complexity of pipe network systems, and the inability of traditional treatment technologies to remove refractory pollutants from the water. At the moment, many researchers are focused on and established a suitable guide for the layout of pipe network systems and predict the water quality problems that may occur in advance and how to solve them (not discussed in this paper) [2–4]. For refractory pollutant removal from drinking water, we found numerous researchers who have developed and applied different methods for their treatment.

This paper reviews the drinking water treatment methods found in the literature (as shown in Table 1); these treatments can be divided into three categories (i.e., physical, chemical, and biological methods). Physical processes [5–7] (e.g., adsorption and filtration) are simple and feasible, separating the pollutants from the liquid phase, and the separated pollutants are kept to be further treated. Chemical methods [8–14] usually involve adding some chemical reagents (e.g., ozone, Fenton's reagent, and chlorine dioxide), which will inevitably produce some toxic intermediate products during the reaction process, inducing secondary pollution. Biological methods [15,16] tend to be highly selective, and the toxicity and non-biological degradation of some organic pollutants causes them to require a longer time and complex equipment to be effectively removed. Due to this, we have shown the high importance of developing green, safe, and efficient technologies for drinking water security assurance. Therefore, micro–nanobubbles (MNBs) used to generate hydroxyl radicals (·OH) with strong oxidation in situ can provide a new approach for the safe and efficient removal of pollutants in the water supply network.

Table 1. Summary of drinking water treatment methods.

Treatment Methods		Pollutants Removed from Drinking Water	Advantages	Disadvantages	References
Physico-chemical methods	Adsorption	Organic pollutants (bisphenol A)	Simple and effective	Adsorbent regeneration and high cost; the adsorption capacity of the regenerated adsorbent decreases, and the service life is short	[5]
	Membrane separation technology	Particles, sediment, algae, bacteria, protozoa, small colloid, virus, dissolved organic matter, divalent ions monovalent ions, and COD	No secondary pollution	High energy consumption, complex equipment, and high intake water quality requirements; membrane fouling	[6]
	Coagulation/flocculation	Refractory organics	Economical and practical	Produce secondary pollution	[7]
	Ultrasonic decomposition	Particles and organic pollutants	Short reaction time and simple process facilities	Relatively low efficiency	[17]
	Photocatalytic technology	Dissolved organic carbon (DOC) and bacteria	Semiconductors are cheap, can mineralize refractory compounds, and are clean and safe	Still in the development stage and immature	[9]
Chemical methods	Electrochemical advanced oxidation processes (EAOPs)	Organic micropollutants	Has environmental compatibility, versatility, high efficiency and safety	Relatively low efficiency; formation of stable by-products	[10,11]
	O_3-based oxidation process	Organic pollutants (chlorophenols) and bacteria	Economical and efficient, harmless to most organisms, and no harmful by-product generation	Harmful to human health; high energy demand	[8,9]

Table 1. *Cont.*

Treatment Methods		Pollutants Removed from Drinking Water	Advantages	Disadvantages	References
Chemical methods	H_2O_2-based oxidation process	Organic pollutants (chlorophenols) and bacteria	Safe, efficient, and easy to use; widely used to prevent pollution and improve biodegradability	The reaction process is affected by many factors, and the reaction time is long	[9]
	Chlorine-based oxidation process	Organic matter, bacteria, micropollutants, and viruses	Chlorine remains in the water as residual chlorine, and the activity is persistent. High yield of active species, broad-spectrum, safe, and effective	Taste and smell are not ideal; forms more than 40 DBPs; disinfection effect is not ideal, and is used for secondary disinfection	[12–14,18]
Biological methods	Biological sand filtration (BSF)	Viruses, bacteria, heavy metals, nitrogenous compounds, pesticides, organic chemicals, dissolved organic carbon (DOC), NOM, etc.	Easy operation, efficient and reliable operation, and low cost	Microorganisms have a high selectivity to pollutants, and the biodegradation time is long, and the equipment is complex; The uncontrolled growth of microorganisms may lead to health problems; The application of biological sand filtration has high requirements on terrain and limited application scenarios.	[19–23]
	Biological activated carbon (BAC)	Nitrogenous compounds, organic carbon, and micropollutants.	The dual functions of adsorption and biodegradation improve the effectiveness of drinking water		[24–28]
	Trickling filter (TF)	NH_3-N, Fe, and Mn	No external air supply required		[29]
	Biological aerated filter (BAF)	COD, NH_4^+-N, Fe, Mn, and diclofenac	Economical and effective		[30–34]
	Membrane bioreactor (MBR)	Nitrate, total organic carbon (TOC), deamination, macropollutants, and anionic micropollutants (perchlorate, bromate, and nitrate)	Overcomes the problem of microbial contamination and supports the growth of selected microorganisms		[35–38]
	Fluidized bed biofilm reactor (FBBR)	TOC, THM, and ammonia	No backwash required and easy to manage		[39]
	Integrated/combining technologies	Microorganisms, particles, nitrate, phosphate, organic matter, and ammonium	Higher treatment efficiency; improve the quality of the treated water and reduce membrane pollution		[40,41]

MNBs are bubbles with a respective diameter of greater than 1 μm and smaller than 1 μm [42]. As a kind of tiny bubble with a diameter in the micrometer or nanometer scale, compared with ordinary bubbles (diameter ≥ 1 mm), MNBs have the characteristics of a small volume, large specific surface area, long existence time, efficient mass transfer ability, high surface potential, high adsorption capacity, and ·OH generation. Additionally, due to the efficient mass transfer ability of MNBs, the dissolved oxygen level in the water is increased, which is conducive to improving the biological activity [42,43]. MNBs have been widely applied in different fields due to their superior characteristics, as shown in Table 2. For example, MNBs have a strong adsorption performance due to their large specific surface area and are extensively used in metal surface cleaning to remove oil stains on the surfaces [44]. According to the high mass transfer efficiency (biochemistry field), MNBs can substantially increase the efficiency of oxygen use for microorganisms and improve aerobic metabolism and microbial growth [45]. The high absolute zeta potential value and high density of NBs may be conducive to nutrient transport and play a positive role in promoting the growth of probiotics, which can be provided using nanobubble water (NBW), to contribute to the production of probiotics [46]. Over recent years, more

and more attention has been paid to the removal process of organic pollutants, refractory pollutants, and pathogenic microorganisms in sewage by MNBs. For example, MNBs have a worthwhile degradation effect on methylene blue in printing and dyeing wastewater, and the ·OH generated during bubble collapse in water plays a significant role in the degradation process of methylene blue [47]. Due to the attributes of ·OH generation in micro–nanobubble water (MNBW), it can significantly inhibit the proliferation of *E. coli* in sewage by 75% under the MNB treatment [48].

Table 2. Application of MNBs in different fields.

Application Fields	Main Function	Gas Type	Bubble Size (nm)	Bubble Concentration (One/mL)	Characteristics of Applied MNBs	References
Biochemical process	Promote the growth of microalgae and increase the output of many high-value products.	Air	<200	/	④	[49,50]
	Improve biofilm structure and promote aerobic metabolism; improve COD and ammonia removal rate and reduce aeration.	Air	<225	/	④	[45,51]
	Improve the production efficiency of probiotics through fermentation, mainly in the lag stage and logarithmic stage of strain growth.	Air	180~220	$(3.59 \pm 1.14) \times 10^7$	⑥	[46]
	Improve the production efficiency and recovery rate of yeast.	Air	$\approx 3 \times 10^5$	/	④	[52]
Groundwater remediation	Improve the mass transfer efficiency of O_3 and the in situ remediation efficiency of organically contaminated groundwater.	O_3	10~1000	$(1{\sim}1000) \times 10^6$	③, ④	[53]
Surface cleaning	Prevent and remove protein adsorbed on solid surface.	Air	25~35	/	⑦	[54,55]
	Remove oil stain on metal surface.	Air	$(2{\sim}6) \times 10^4$	/	①, ②	[44]
Agronomy	Improve irrigation water use efficiency, crop yield, and quality.	Air	124~148	$(6{\sim}7) \times 10^8$	④	[56]
	Improve plant growth; purify blue-green algae pollution.	Air	200~2200	/	④	[57]
	Change the redox conditions of submerged paddy soil to reduce methane emission.	O_2	128~242	$(6{\sim}8) \times 10^7$	④	[58]
Soil environment	Remove metal pollutants from soil.	O_2	$<10^3$	/	④	
	Improve the availability of oxygen in clay or sandy soil and improve the soil anoxic environment.	O_2	190~210	$(0.5{\sim}1.5) \times 10^9$	④	[59]
Marine animals and food	Significantly promote the growth of plants, fish, and mice.	O_2 Air	<200	/ /	④	[60]
	Aeration to improve oxygen mass transfer efficiency.	Air	$10^2{\sim}10^5$	/	④	[61]
Water pollution treatment	Disinfect and can effectively remove bacteria and viruses.	O_3	$(3{\sim}6) \times 10^4$	/	⑤	[62]
	Flotation to improve the treatment effects of printing and dyeing wastewater.	Air	$<6 \times 10^4$	/	②, ③, ④, ⑤	[63]
	Degradation of organic pollutants					

Note: ①, small volume; ②, large specific surface area; ③, long existence time/good stability; ④, good mass transfer efficiency; ⑤, hydroxyl radical generation; ⑥, high absolute zeta potential value and high NB density; ⑦, NBs occupy protein adsorption sites.

Advanced oxidation processes (AOPs) have recently caught the attention of numerous scientists because of their characteristics to degrade pollutants in water through ·OH generation in the reaction. ·OH is significantly oxidizing (standard redox potential is higher at 2.85 V, second only to F_2), and can rapidly oxidize almost all organic matter until mineralization. The process to generate ·OH is complex when using traditional advanced oxidation technologies (e.g., ozone oxidation, chemical oxidation, and electrochemical

oxidation) due to the number of chemical agents or catalysts that need to be added to the reaction system. As a result of this reaction, a significant secondary pollution risk can be induced in the water treatment process. For instance, for the catalytic oxidation process of ozone, various dissolved metal catalysts (Zn^{2+}, Mn^{2+}, and Cu^{2+}) or solid metal catalysts (TiO_2, MnO_2, and Al_2O_3) need to be added to the reaction. The use of these catalysts not only increases the cost of the water treatment, but also has the possibility of metal leaching, which leads to certain risks and challenges to water treatment [64]. Based on this, this method can be widely applied to sewage treatment. For drinking water, the essential standards, such as water quality and sensitivity, cannot be solved using a traditional AOP for its treatment. Therefore, generating ^-OH safely, greenly, and efficiently has become a grave bottleneck problem that restricts the development of AOPs in drinking water treatment.

Compared with the traditional ·OH generation methods, ·OH can be generated by MNBs in the process of dissolution and collapse without adding any chemical agents or catalysts [65], which has the advantages of cleanliness, safety, and environmental protection. It is very suitable for ensuring the safety of drinking water with high water quality standards and a high sensitivity. Therefore, MNB technology has gradually shown potential in drinking water treatment applications; however, its technology has barely been tested for the drinking water security field. The main reasons can be defined as follows: (i) it is difficult to obtain stable MNBs in water; (ii) it has a low efficiency of ·OH generation by MNBW; and (iii) the removal efficiency of pollutants cannot be guaranteed. In order to solve these issues, this paper focuses on reviewing the generation process and particle size characteristics of MNBs in water. Mostly, the process is to obtain stable and controllable MNBW using physical or chemical methods. Thus, we sort out the bubble collapse and ·OH in situ generation process and its influencing factors in MNBW to analyze its potential application for drinking water safety by combining the removal mechanisms of pollutants and pipe wall biofilm. Based on this method, the MNB technology provides an innovative theoretical basis and technical support for solving the problem of drinking water safety.

2. Generation Process and Characteristics of MNBs in Water

2.1. The Generation Process of MNBs in Water

The continuous and stable generation of a large number of MNBs is the premise and basis for the broad application of its technology in various fields; hence, it is crucial to understand how to generate MNBs in water. In this section, we deeply describe the methods to produce MNBs in water. By comparing different occurrence conditions and equipment structures of MNBs, a suitable guide to carry out the stable generation of MNBs in the drinking water treatment process and improve the feasibility of its technology is produced. Table 3 summarizes ten methods for generating MNBs in water and provides an overview of their advantages and disadvantages.

According to Table 3, the generation methods of MNBs can be summarized into two categories (i.e., mechanical and chemical). The mechanical methods are based on mixing up water and gas by increasing pressure. Then, by applying high-speed rotation, impact, and cutting, the water–gas mixture releases high-density MNBs in an instantaneous dispersion, which can be obtained by increasing saturation pressure, bubble shear, cracking, and mechanical stirring without any catalyst [65]. Chemical methods usually require chemical or electrolytic reactions to generate MNBs, which differ from mechanical processes due to their strong dependence on chemical reagents and catalysts. Moreover, this process produces uncontrollable by-products, which cause secondary pollution to the water quality environment if it is applied to the field of water purification. For practical cases, the mechanical way of simple operation, cleanliness, and safety is often used to generate MNBs, finding that most methods include ultrasonic cavitation, hydrodynamic cavitation, pressurized dissolved gas release, and the dispersed air method. Various investigations have further explored the influencing factors of the MNB process that are generated using different mechanical techniques, such as the effects of ultrasonic time, ultrasonic

cavitation time, and ultrasonic frequency, which increase the number of NBs generated using ultrasonic cavitation [66]. Using the pressurized dissolved gas release method, it was found that the diameter and quantity density of the generated MBs depended on the cavitation mode of the nozzle, analyzing the liquid volume flow influence (decompression nozzle), and dissolved gas concentration upstream of the nozzle [67].

Table 3. Summary of different micro–nanobubble generation methods.

Generation Methods	Generation Process	Influence Factor	Advantages	Disadvantages	References
Hydrodynamic cavitation	When a large pressure difference is generated in the moving fluid, hydrodynamic cavitation will be observed, resulting in MNBs.	Pressure difference	High efficiency and low energy consumption	Bubble size is not easy to control	
Ultrasonic cavitation	A sound field is applied to make the liquid generate tensile stress and negative pressure. If the pressure is too saturated, MBs will be generated.	Ultrasonic time, frequency	The bubble size is small and uniform	Complex operation for large-scale treatment	
Optic cavitation	A certain wavelength of light is irradiated on the photocatalysis material, which makes the electrons transit, and MNBs precipitate.	Wavelength of light	No secondary pollution	High cost and not conducive to mass production	
Jet dispersion method	The air–liquid mixture is formed after the air compressor is injected or inhaled by itself and then injected at high speed, relying on the turbulence between the air and liquid to generate MNBs.	Air intake	Rapid generation of MNBs with uniform size	The air intake is difficult to control	
Compressed air passing through diffusion plate method	The pressurized air enters the liquid phase through the micropores with a certain size on the special diffusion plate, and the gas forms MNBs under the shear of the micropores.	Size of micropore	Relatively simple operation and easy to form MNBs	Expensive device, and pores are easy to block	[43,67–69]
Mechanical force high-speed shearing air method	The larger bubbles in the liquid are divided into MNBs by using the shear effect generated by the high-speed rotating impeller.	Impeller rotation	Rapid generation of a large number of MNBs	Unstable bubble size and high energy consumption	
Dissolved gas release method	First, the gas is pressurized to supersaturate and dissolve it, and then is decompressed to be released, thus producing MNBs.	Pressure and nozzle cavitation mode	Simple operation and low energy consumption	Discontinuous gas dissolution and release and low efficiency	
Aeration method	Various micro–nanobubble generators are directly used to aerate in water, producing MNBs.	MNB generator type	Easy to operate, non-toxic, and residue free	The instrument is expensive	
Chemical reaction method	Chemical reagents are added to the solution to make it react violently, producing MNBs.	Type of reactant	High bubble generation efficiency	Cause secondary pollution	
Electro-chemical method	Water is electrolyzed through electrodes to form MNBs on the positive and negative plates.	Voltage size and electrolytic time	The size of bubbles can be controlled	High energy consumption and low efficiency	

MNB generation devices are based on the abovementioned mechanical methods, which have been industrialized for their application. Moreover, there are four types of mature generators: pressure dissolving type, vortex type, Venturi type, and jet type, which have different efficiencies in producing MNBs. Among them, the pressure dissolving type micro–nanobubble generator (MNBG) uses the principles of the pressurized dissolved

gas release method to generate MNBs. The production efficiency of MNBs is low due to the discontinuity of the gas dissolution and release processes. A vortex-type MNBG utilizes high-speed crushing and shear interactions between gas–liquid mixtures to form MNBs. Wu et al. reported the efficient generation of MNBs under low energy consumption conditions using the self-developed vortex-type MNBG [70]. According to numerous scientists, the Venturi type MNBG is highly used due to its simple structure, high efficiency of bubble generation, and low energy consumption. Li et al. studied the influence of the main parameters of the Venturi bubble generator, such as its injection hole diameter, injection hole number, and divergence angle, on the bubble generation process in water [71]. The results showed that the divergence angle is the central parameter controlling the bubble size, and the larger the divergence angle, the smaller the bubble size. Zhao et al. further studied the mechanism of influence of the divergence angle on the bubble size, revealing that the bubble might experience a drastic deceleration in the divergence stage of the Venturi channel [72]. Due to the large divergence angle, the bubble velocity will decrease and extend the time of the powerful interaction between the gas and liquid phases, which makes it stretch and deform, causing the bubbles to burst and create more and smaller bubbles. The design of a jet-type MNBG takes advantage of the Venturi effect. The fluid channel first converges and then expands. In the convergence stage, the fluid pressure energy is converted into velocity energy, creating a low-pressure area; thus, gas is self-aspirated from the highly reduced pressure point. The gas–liquid mixture enters the diffusion stage through the throat of the injector, reducing the velocity; afterward, the MNBs are generated by the turbulence and shear effect between the gas and liquid. Thus, using a liquid ejector instead of a traditional agitator, the vibration of the agitator can be avoided, which has the advantage of a low equipment maintenance cost.

According to the above criterion, there are various types of MNB generation methods in water. Nevertheless, it is hard to obtain bubble water with a stable particle size distribution using either mechanical or chemical methods; hence, the size distribution of bubbles in water is immense, ranging from tens of nanometers to tens of micrometers. Based on previous approaches, the bubble generation process is limited to the mechanical process of bubble cutting, and there is no scientific unified consensus on the stable generation and existence mechanism of bubbles. Therefore, the scientific community refers to this kind of water containing MBs and NBs as MNBW. It is worth mentioning that different generation methods and test conditions influence the MNB quantity and characteristics and affect the effectiveness of MNB technology in drinking water treatment applications. By exploring and optimizing the stable generation mechanism, the occurrence conditions and equipment structure of MNBs can guarantee the effective generation of MNBs, improving the quality and quantity of MNBs in drinking water treatments. The MNB generation process in water is shown in Figure 1A.
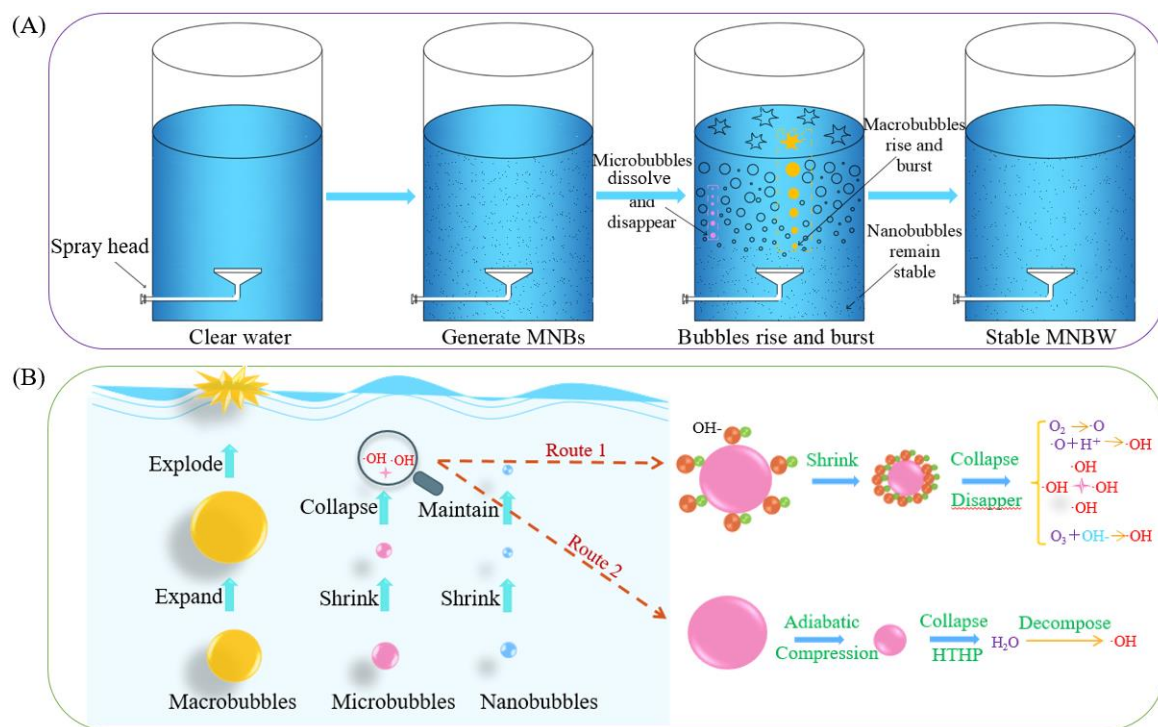
Figure 1. Differences among microbubbles, microbubbles, and nanobubbles. (**A**) The generation process of micro–nanobubbles in water. (**B**) Mechanism of hydroxyl radical generation by micro–nanobubbles. Note: HTHP, high temperature and high pressure.

2.2. Characteristics of MNBs in Water

It is crucial to analyze the MNB characteristics, which have been widely applied in various aspects. Compared with ordinary bubbles, MNBs have the characteristics of a small volume, large specific surface area, long existence time, efficient mass transfer ability, high surface potential, strong biological activity, high adsorption capacity, and ability to generate ·OH, as described in detail below.

(1) Long existence time: After generating ordinary bubbles (diameter ≥1 mm) in water, they can rapidly rise to the surface, rupture, and disappear, making their existence time very short in water. Compared with ordinary bubbles, the existence time of MNBs is significantly longer in water, and the process from generation to collapse usually lasts tens of seconds or even minutes [73]. Moreover, for MBs, the smaller the volume is, the slower the rise rate in water is, and the longer the existence time is. For NBs [74], they can exist for several weeks after being generated in water, as shown in Figure 1 and Table 4.

Table 4. The differences among macrobubbles, microbubbles, and nanobubbles.

	Macrobubbles	Microbubbles	Nanobubbles	References
Size	>100 μm	1–100 μm	<1 μm	
Specific surface area	Small	Large	Larger	
Buoyancy force	Large	Small	Smaller	
Existence time	10^0–10^1 s	10^1–10^2 s	>10^5 s	
Rising velocity	>10^4 μm/s	10^1–10^3 μm/s	<10^0 μm/s	[43,65]
Mass transfer efficiency	Low	High	Higher	
Zeta potential	/	−50 mv–10 mv	<−50 mv	
Formation of hydroxyl radicals	/	Yes	Yes	
Internal pressure	Low	High	Higher	
DO level	<10^0 mg/L	10^0–10^1 mg/L	>10^1 mg/L	

The stability mechanism of NBs in water has played a crucial role in the longtime existence of MNBs in water. Therefore, this paper summarizes the mechanism and reasons for the stable existence of NBs in water. Firstly, MNBs' sizes are smaller, inducing their buoyancy in the water, which makes them rise very slowly and steadily through the water. For instance, for bubbles with a radius of 100 nm, the rising speed in water is around 20–30 nm/s [75]. MNBs with a diameter of less than 1 μm rise much slower in water than by using the Brownian motion [76]. The inner density of a bubble at the nanoscale may be very high, even close to the liquid density of gas, which increases the NBs' life by four orders of magnitude [77]. It is worth pointing out that the density inside the bubble increases with a decrease in the bubble size, indicating more stability with a small size. By measuring the angle corresponding to the liquid phase adjacent to the NBs, which is well known as the contact angle, it was found that compared with the macroscopic bubbles, the contact angle and radius of curvature of the NBs are much larger, and the corresponding Laplace pressure driving bubble dissolution was reduced, which greatly improved the stability of the NBs in solution [78]. The strong hydrogen bond presence at the NBs' interface in water further increases the stability of the NBs, whose structure is different from that of bulk water, and it can keep NBs stable at lower internal pressures [75,79]. To explore the bubble interface characteristics, it can be found that a large number of OH- ions accumulate on the surface of MNBs, inducing a high negative zeta potential, and the repulsive force between the negative charges prevents the merging of NBs [80]. The surface of NBs is partially covered by hydrophobic impurities (e.g., oil, fat, and carbon particles) that further aggravate the resistance of the bubble merger [81,82]. Thus, the nanoscale particle size and particular interfacial properties of the bubble allow for the NBs in water to show a high stability and durability.

(2) Efficient mass transfer ability: As a terminal electron acceptor of microorganisms, dissolved oxygen (DO) plays an important role in aerobic biodegradation. Compared with ordinary bubbles, MNBs contribute to the increase in the DO concentration in water due to their efficient mass transfer ability [43]. It was found that the mass transfer efficiency of MBs with an average particle size of 33 μm was much higher than that of ordinary bubbles with an initial particle size of 10 mm. The dissolved oxygen peak value (DOPV) and the average initial dissolved oxygen increase rate (AIDOIR) of oxygen MBs were 100 times and 2 times higher than those of ordinary oxygen bubbles, respectively. The DOPV and AIDOIR of air MBs were 35 times and 1.05 times higher than those of ordinary air bubbles, respectively [61]. The DO mass transfer rate of oxygen MNBs was 125 times higher than that of ordinary air bubbles. Meanwhile, the highest DO peak was 3 times higher [83]. The DO concentration produced by MB aeration was 9.87 mg/L in 60 min, while the DO concentration produced by ordinary aeration was only 6.54 mg/L in 100 min under the same airflow condition [84]. The oxygen utilization rate and volume mass transfer coefficient of the MNB aeration system were about twice as high as that of the ordinary bubble aeration system [85].

Generally, the mass transfer rate of the gas phase depends on the mass transfer area of the gas–liquid phase and is positively correlated with it; MNBs have shown a high mass transfer because of their large mass transfer area. According to Henry's law, when the bubble diameter is small, the surface tension makes the MBs shrink continuously due to them undergoing self-compression and dissolution in water, making the dissolution rate of gas in water reach supersaturation, improving the mass transfer efficiency [86,87]. This statement can be explained by the Laplace equation, which is defined as follows:

$$\Delta P = 2\gamma/R \tag{1}$$

where ΔP is the pressure difference between the inside and outside the bubble, γ is the surface tension of the interface between the bubble and the surrounding liquid, and R is the bubble radius. Interestingly, with a smaller bubble size, the internal pressure and specific surface tension increase significantly, permitting the gas to pass through the bubble interface and dissolve into water, which is conducive to the gas–liquid mass transfer.

Moreover, with a high difference in the pressure between the inside and outside of the bubble, the mass exchange from the bubble to the water will be faster [88]. Notably, when MNBs rise very slowly and have a stable existence in water and prolong the gas–liquid mass transfer time, the gas–liquid mass transfer might be elevated.

(3) High adsorption capacity: MNBs have a large specific surface area due to their small volume; thus, the contact area with pollutants is also extensive, significantly improving the adhesion probability between the contaminants and bubbles. These compounds (pollutants) are adsorbed on the interface of the MNBs, where they are degraded by oxidants or rise to the water surface with the MNBs. With a pH of 8, due to the contact promotion between aromatic hydrocarbons and ·OH at the MNB interface, the oxidation efficiency of ozone MNBW for aromatic hydrocarbons increased by 13.6–22.6% compared with ozonized water [89]. Compared with conventional macrobubbles, oil easily adheres to the surface of the MNBs due to the large specific surface area per unit volume of liquid, and due to the low density, oil can rise to the surface with MNBs by flotation for oil collection and oil–water separation [90]. With the assistance of deionized water, MNBs successfully removed 80–90% of the oil on the surface of metal parts, and had the advantages of low energy consumption, sustainability, efficiency, and being green [44].

(4) Generation of ·OH: MNBs have been widely applied for water treatment due to their ·OH generation and powerful oxidizing capacity. Many studies have confirmed that free radicals, including ·OH, are generated in the MNB collapse process. Recently, the mechanism of MNBs generating free radicals has not been deeply studied, but can be summarized into two theories: the ion accumulation theory and adiabatic compression theory induced by ultrasonic cavitation or hydrodynamic cavitation. With regard to the former, in the absence of dynamic stimulation, the high concentration of ions accumulated at the gas–liquid interface and the accumulated chemical energy play an important role in the generation of ·OH and alkyl radicals during the MB collapse process [91]. By studying the degradation of methylene blue by MBs, it was also shown that in the absence of any dynamic stimulation, air MBs could continuously generate a large number of ·OH, in which the decomposition of oxygen molecules caused by the rapid increase in the absolute value of the zeta potential at the gas–liquid interface was the key to the generation of free radicals. And the higher air flow rate and lower pH were favorable to highly increase ·OH generation [47,92]. Ozone MBs reacted with OH- at the gas–liquid interface to generate ·OH [92]. As shown in path 1 in Figure 1B, the above research reports all support the ion accumulation theory.

On the other hand, the adiabatic compression theory describes that when water is exposed to ultrasonic radiation, a higher number of tiny bubbles appear and burst violently, which is well known as the acoustic cavitation phenomenon [91]. These tiny bubbles repeatedly expand and contract according to the incident ultrasonic wave pressure oscillation. If the bubble contraction speed exceeds the speed of sound, the internal temperature of the bubble will rise sharply due to the adiabatic compression when it bursts. All of this can establish a high hot spot. As previously stated, the internal pressure of MNBs is inversely proportional to their particle size, indicating that a small particle size increases the internal pressure. Therefore, a high pressure point will also form in the final stage of the contraction and collapse of MNBs. Under this extremely high temperature and pressure condition, MNBs collapse, and ·OH is generated, as shown in path 2 in Figure 1B. When high-frequency (1650 kHz) ultrasonic waves were irradiated into water dissolved with different gas molecules, free radicals were generated, and the generation mode of free radicals was determined by the dissolved gas molecules [93].

Due to the strong oxidation capacity of ·OH, MNB technology plays a crucial role in the removal process of refractory organic matter. We used MNBW to treat the phenol solution and found that the degradation rate of phenol was as high as 52.8%. After adding tert-butyl alcohol to quench the ·OH, the degradation rate of phenol was only 11.1%. Moreover, the DMPO-OH was detected using an electron spin method, which fully showed that ·OH was generated in MNBW, as shown in Figure 2A. Notably, the number and type of free

radicals generated during the collapse of MNBs are also affected by diverse factors, such as the gas type, pH value, temperature, bubble size, etc., which will be discussed in detail in Section 2.2.

(5) High zeta potential: According to the theory of a compressed electric double layer, the MNB surface adsorbs negatively charged surface ions and positively charged countercharged ions due to the electrical attraction. The zeta potential is commonly used to characterize the potential difference in the surface charge formation of MNBs, indicating that is essential to determine the interaction of bubbles during the merging process and the method of interaction between the bubbles and other materials [94]. When MBs contract in water, the charged ions are rapidly concentrated and enriched at the very narrow bubble interface, inducing a significant increase in the zeta potential. A very high absolute zeta potential value can be produced at the interface before the bubble collapses [91]. Moreover, the smaller the particle size of MNBs, the higher the concentration of ions aggregated per unit area, and the higher the zeta potential produced. Takahashi reported the zeta potential of the MNB surface in an aqueous solution and found that MBs were negatively charged under a wide range of pH conditions, but positively charged only under strongly acidic conditions [95]. For example, in distilled water at pH 5.8, air MBs were negatively charged with an average zeta potential of about -35 mv. With the increase in the pH value, the absolute value of the zeta potential increased until it reached a stable value of about -110 mV at pH 10. It was also proved that OH^- and H^+ were the key factors affecting the charge at the gas–water interface. In addition, many studies have confirmed that the zeta potentials of different MNBs are negative, but their absolute values change with the type of gas in the MNBs, the pH of the solution, and the type and concentration of the electrolyte solution [96–98].

Based on this, it is worth noting that the various characteristics of MNBs are not unrelated, but consistent and codependent, as shown in Figure 2. With a smaller MNB size, the adsorption capacity, the zeta potential, and the existence in water is significantly elevated, which is more conducive to improve the gas–liquid mass transfer and the biological activity of the MNBs (as shown in Figure 2B–D). An increase in the Zeta potential on the surface of MNBs plays a crucial role in the formation of $\cdot OH$ during its collapse; additionally, it is beneficial to the stable existence of MNBs in water. By analyzing the factors that affect the MNBs' stability, the results showed that MNBs with a high negative zeta potential could be generated in a solution with a high pH value, low salt concentration, and low temperature. And the bubbles generated under alkaline conditions were smaller and more stable, while those generated under acidic conditions were larger and more unstable [98]. Hamamoto et al. confirmed that MNBs were more stable under alkaline conditions [99]. This can be explained by the fact that at a higher pH and in the presence of a higher OH^- concentration, the MNBs' surface charge becomes more negative, the zeta potential is higher, and the repulsion between bubbles is greater, hence, more stable. In particular, it is because of these closely related MNBs characteristics that its technology shines brightly in different fields.
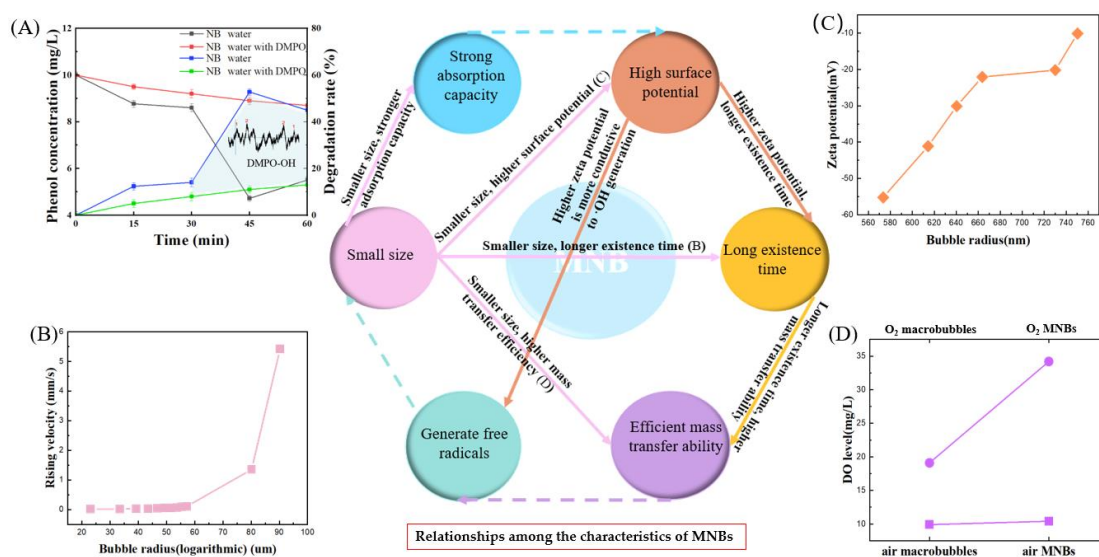
Figure 2. Relationships among the characteristics of MNBs. (**A**) Degradation of phenol by MNBW. (**B**) The relationship between the bubble rising velocity and bubble radius indirectly reflects the relationship between the bubble rising velocity and existence time. (**C**) The relationship between the bubble zeta potential and bubble radius. (**D**) The relationship between the DO level and bubble radius indirectly reflects the relationship between the bubble mass transfer efficiency and bubble radius. (Ref. [61], (**B**): reproduced with permission from [Li Hengzhen et al.], [Water Environment Research]; published by [WILEY], [2014]; Ref. [100], (**C**): reproduced with permission from [Li Hao], [Jiangsu University]; published by [Jiangsu University], [2020]; Ref. [83], (**D**): reproduced with permission from [Li Hengzhen et al.], [International Journal of Environmental Research and Public Health]; published by [MDPI], [2014]). Note: Solid line means established relationship, dotted line means relationship unknown. (i) TB means for tert-butanol, ·OH quencher. Experimental conditions: temperature 15 °C, pH 7.3, and initial concentration of phenol 10 mg/L.

3. Characteristics of MNB Collapse and Influencing Factors of Hydroxyl Radical Generation in MNBW

3.1. Characteristics of MNB Collapse

The growth and collapse of MNBs is accompanied by changes in the bubble morphology and surrounding microenvironment. A complete bubble period is divided into three phases: growth, collapse, and post-collapse [101]. During the growth phase, the bubble slowly expands (lasting tens of milliseconds); during the collapse phase, the bubble rapidly shrinks (lasting more than ten microseconds). In the process of bubble growth and collapse, the bubble generates microjet and shear stress on the surrounding fluid, forming a local high temperature and pressure point, which induces the ·OH generation under the extreme environments of a high temperature and high pressure. In the post-collapse phase, the fluid gradually returns to its original state under the actions of the previous two phases. Kröninger et al. analyzed the collapse process of MBs through high-speed photography, finding that the bubble expanded to a maximum radius of 750 μm at 70 μs, and collapsed for the first time at 140 μs [102]. The team further used particle tracking velocimetry to study the influence of MB collapse on the surrounding flow field, and found that shortly before the bubble collapsed, a ring vortex formed near the bubble wall, and a high-speed liquid jet was produced after the bubble collapsed. The discovery of this high-speed jet is consistent with the results of a 2007 study by Zwaan's team, which showed that the bubbles expanded faster than they contracted. Meanwhile, high-speed jets were generated when bubbles collapsed at the scale of 100 microns near the wall [103].

To compensate for the uncertainty of the morphology test results, scientists promote using numerical simulation methods to quantitatively study the environmental conditions of MNB collapse, of which we are more concerned about the high-temperature and high-

pressure points formed by the MNB collapse. Yasui et al. proposed to use the bubble dynamics model to calculate the high-temperature and high-pressure points, and this model had been verified using the single-bubble sonoluminescence model and sonochemical studies [82,104–106].

$$\frac{d_{ni}}{dt} = -4\pi R^2 D_i \frac{(c_{s,i} - c_{\infty,i})}{R} \tag{2}$$

Here, n_i refers to the number of gas molecules in a bubble, t refers to the time, R refers to the instantaneous radius of a bubble, D_i refers to the diffusion coefficient of gas i in the liquid, $c_{s,i}$ refers to the saturation concentration of gas i in the liquid at the bubble wall, and $c_{\infty,i}$ refers to the concentration of gas i in the liquid away from the bubble, It is assumed that the bubble surface is clean and not covered by hydrophobic materials.

$$D_i = B_i e^{-\frac{\nabla E_i}{R_g T_{L,i}}} \tag{3}$$

Here, R_g is the gas constant, and $T_{L,i}$ represents the liquid temperature at the bubble wall.

$$c_{s,i} = \frac{10^3 \rho_{L,i} N_A P_g}{K_{H,i} M_{H_2O}} \left(\frac{n_i}{n_t}\right) \tag{4}$$

Here, $\rho_{L,i}$ refers to the instantaneous liquid density at the bubble wall, N_A represents Avogadro's constant, P_g refers to the instantaneous pressure inside the bubble, $K_{H,i}$ is Henry's law constant of gas type i under the instantaneous liquid temperature at the bubble wall, which is a function of the temperature, M_{H2O} expresses the molar mass of water, n_i is the instantaneous number of molecules of gas type i in the bubble, and n_t represents the instantaneous total number of molecules in the bubble.

Based on the finite element simulation method, the growth and collapse processes of MNBs are simulated by using the fluid dynamics governing equation and the volume of fluid (VOF) model, and the temperature and pressure changes during bubble collapse are investigated. It was found that the oxygen NBs dissolved in water would generate ·OH due to the high temperature and pressure (2800 K and 4.5 GPa) in the moment. Moreover, ·OH might be generated when the temperature and pressure inside the air NBs increase to about 3000 K and 5 GPa, respectively [82]. Some investigations reported that in this process, if the temperature rises to >5000 K, the water vapor and non-condensable gases (including air) in the bubble will decompose and generate free radicals (such as ·OH) [91]. Wang et al. described that due to the inertia and compressibility of the bubble contents, an immense implosion force might be generated when the bubble collapses, causing local hot spots and releasing a large amount of energy, with a high temperature (500–15,000 K) and pressure (100–5000 Pa) [107]. Sun et al. confirmed that the high hot spot temperature formed by the bubble collapse ranged from 2000 to 6000 K [108]. Currently, there is no consensus on the high-temperature and high-pressure points created by the collapse of MNBs, as shown in Table 5.

Table 5. Temperature and pressure at the time of MNB collapse.

Bubble Type	T	P	Reference
MNBs	>5000 K	/	[91]
Air NBs	3000 K	5 GPa	[82]
Oxygen NBs	2800 K	4.5 GPa	
MNBs	500~15,000 K	100~5000 Pa	[107]
MNBs	2000–6000 K	/	[108]

Based on the above, MNBs produce an extreme environment of high temperature and high pressure when they collapse, generating ·OH in these conditions. The author believes that ·OH generation should involve substances containing two elements of hydrogen and oxygen in water, such as water molecules, hydroxide ions, or organic compounds

containing hydrogen–oxygen bonds. The chemical bond related to hydrogen and oxygen in the substance is broken under a high temperature and pressure to generate ·OH, and the number of ·OH generated may be related to the concentration of the substance containing the hydrogen–oxygen bonds or the ambient temperature and pressure, where the higher the concentration of substances containing hydrogen–oxygen bonds, the higher the energy released during the bubble collapse, and the more hydroxyl radicals that may be generated, even though this speculation needs further studies to confirm it.

3.2. Influencing Factors of ·OH Generation in MNBW

Existing conventional advanced oxidation techniques generate free radicals with the risk of catalyst dependence and creation of disinfection by-products. Their application to sewage treatment is acceptable, but in regard to drinking water quality, the standard is high and sensitive. The presence of catalysts and disinfection by-products will aggravate the water quality sensitivity and threaten the water quality health. Although the MNB technology is green and safe, the free radical generation efficiency is low, and its utilization in drinking water is still limited to a certain extent. Therefore, we are required to deeply explore the free radical generation mechanism and its influencing factors in MNBW, which improves the generation efficiency of ·OH and replaces other advanced oxidation technologies for water treatment. The mechanism of ·OH generation by MNBs has been discussed in the above sections. To enhance ·OH generation by MNBs, it is essential to understand the factors that affect the concentration of ·OH in MNBW. Existing studies have discussed the effects of the pH, gas type, bubble size, temperature, and external stimuli on the production of ·OH by MNBs, as shown in Figure 3A.
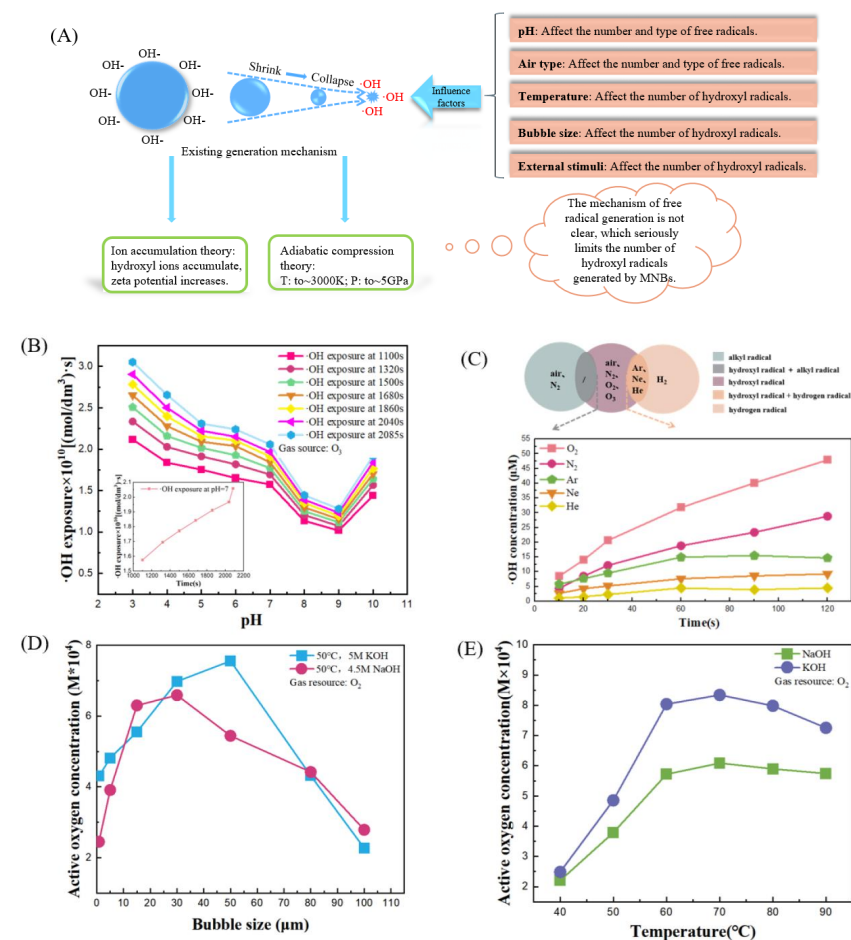

Figure 3. Influence of different factors on the generation of ·OH by MNBs. (**A**) Factors affecting the generation of ·OH by MNBs. (**B**) Effect of pH on ·OH exposure. (**C**) Effect of gas source type on the

generation of free radicals by MNBs. (**D**) Relationship between active oxygen concentration and bubble size. (**E**) Relationship between active oxygen concentration and temperature. (Ref. [109], (**B**): reproduced with permission from [Snigdha Khuntia et al.], [Chemical Engineering Research and Design]; published by [ELSEVIER], [2015]; Ref. [93], (**C**): reproduced with permission from [Masahiro Kohno et al.], [Journal of Clinical Biochemistry and Nutrition]; published by [The Society for Free Radical Research Japan], [2011]; Ref. [110], (**D,E**): reproduced with permission from [Yu Xiaobin et al.], [Journal of Chemical Technology & Biotechnology]; published by [WILEY], [2017]).

(1) pH: The pH affects the generation of free radicals by MNBs from two aspects: the type of free radicals generated by MNBs and the number of ·OH generated by MNBs. First, we reviewed the current research on the effect of the pH value on the type of free radicals generated by MNBs. Takahashi et al. found that MNBs in distilled water could generate alkyl radicals during the rupture process [91], which may be caused by the presence of trace organic pollutants in the water, using electron spin resonance spectroscopy and a DMPO spin capture agent. ·OH might be observed under strongly acidic conditions, because the pH impacts the charge of the gas–water interface, where the zeta potential of the MNBs changes from negative to positive. The type of ions accumulated at the interface during collapse may be related to the type of free radicals generated. Li et al. (2009a) tested the electron spin resonance method to study the free radical types generated by MNB collapse [111]. Using this method, it was found that the presence of trace organic pollutants in distilled water containing nitrogen MNBs may induce the generation of alkyl free radicals. When the pH was reduced to 2.3, ·OH was generated in solutions containing either nitrogen or oxygen MBs. The above studies indicate that the pH can affect the type of free radicals generated by MNBs.

Second, the pH affects the number of ·OH generated by the MNBs. It is generally accepted that the increase of hydroxide ions at high pH is beneficial for ·OH generation. In an ozone MNB aqueous solution [112], ·OH was assumed to be generated by the interactions between the ozone and hydroxide ions which were gathered at the bubble interface during the collapse of the MBs. Hence, a higher pH value and hydroxide ion concentration induce more favorable conditions for the generation of ·OH. Similarly, it has been suggested that the free radical chain generating ·OH is stimulated by chemical reactions between the ozone and hydroxide ions. Thus, high pH conditions induce ·OH generation in ozone systems [113]. However, in the absence of an accepted explanation, various experiments have also shown the opposite effect of favoring ·OH generation under strongly acidic conditions, which can be induced by the addition of hydrochloric, sulfuric, and nitric acids. Takahashi et al. used electron spin resonance spectroscopy to show that a large number of ·OH might be generated when ozone MBs burst in strongly acidic aqueous solutions [112]. Using the spectral characteristics of DMPO-OH, formed by DMPO and ·OH, it was concluded that oxygen MBs generated more ·OH under acidic conditions [114]. The experiment of phenol degradation by MNBs and the remarkable improvement in the phenol degradation rate under acidic conditions also proved this. It has been reported that ·OH is formed after the reaction between the oxygen atoms and is produced by the decomposition of oxygen molecules and protons, so a high oxygen concentration or low pH is conducive to the generation of ·OH [47]. Khuntia et al. tested p-chlorobenoic acid (PCBA) as the probe compound to quantify and predict the ·OH generated by ozone MBs [109]. The results showed that the exposure value of ·OH decreased with an increase in the pH from 3 to 9, but increased at pH 10 due to the increase in the hydroxide ion concentration of the solution and continued to increase with time, as we can see in Figure 3B.

(2) Type of gas source: Similarly to the pH, the type of gas source also affects the kind of free radicals and the number of ·OH generated by MNBs, as shown in Figure 3C. Regarding the former, Kohno et al. used electron spin resonance spectroscopy and DMPO as a spin trapping agent to study the free radicals generated by the ultrasonic cavitation of water samples dissolved with different gases [93], and found that the generation of free radicals was related to the type of gas in MNBs, and only ·OH was generated during

oxygen MB collapse. In addition, only hydrogen free radicals were generated during hydrogen MB collapse, while ·OH and hydrogen free radicals were generated during nitrogen MB collapse. For noble gas MBs, ·OH and hydrogen free radicals were generated during the collapse process, which indicated that the type of free radical generated by MNBs was related to the type of gas. Furthermore, the results showed that the oxygen MBs generated more ·OH than nitrogen MBs. The number of hydrogen radicals and ·OH generated by the noble gas MBs increased in the order of Ar > Ne > He [93]. These findings are consistent with their earlier report [115] on noble gas MBs. The number of ·OH generated during the collapse process increased in the following order: Xe > Kr > Ar > Ne > He. They interpreted these results as such: the generation of ·OH increased as the thermal conductivity of the noble gas decreased and as the final temperature of the collapsed cavitation bubble increased. Li et al. analyzed the effect of changing the type of gas supplied to the microbubble generator on phenol degradation [114]. It was found that during the two-hour treatment, the degradation rate of phenol increased in the following order: nitrogen < air < oxygen, 36%, 59%, and 83%, respectively. Moreover, the detection using electron spin resonance spectroscopy showed that ·OH was generated by oxygen MB collapse, and the decomposition of oxygen was the key to the free radical generation, while ·OH was generated by air and nitrogen MBs only under acidic conditions. Therefore, oxygen MBs are the most conducive to the generation of ·OH, followed by air MBs and nitrogen MBs. Since ozone is involved in the reaction of ·OH generation during MNB collapse, the ozone MNBs can be considered to promote ·OH generation. Hu and Xia applied MNBs to degrade methyl orange, and the results showed that the degradation rate of methyl orange by ozone MNBs was much higher than that by oxygen MNBs, indicating that ozone MBs were more conducive to the generation of ·OH than oxygen MBs [53].

Thus, the gas type can affect the free radicals generated by MNBs. For the impact on the number of ·OH generated by MNBs, the production of ·OH generated by the collapse of noble gas MNBs increases in the order of Xe > Kr > Ar > Ne > He. The production of ·OH generated by the collapse of non-noble gas MNBs increases in the order of ozone > oxygen > air > nitrogen.

The pH value and gas type have a crucial effect on the generation of ·OH by MNBs, which are closely related and can also be considered together.

(3) Bubble size: The bubble size also plays a crucial role in the generation of ·OH by MNBs. Yu et al. reported that titanium microporous filters to control the size of MNBs can be used to study the effect of their size on the concentration of reactive oxygen species (ROS) [110]. The results showed that the dependence of the ROS concentration on the size of microporous filters induced a quasi-parabolic change. This is because with the increase in the MNB size, the stability of the bubbles is reduced, and the bubbles are more likely to collapse, which is conducive to the formation of ROS, while the surface charge density of the bubbles is reduced, which is not conducive to the formation of ROS. Therefore, the dependence of ROS formation on the bubble size is a balance between the bubble surface charge density and bubble stability, as we see in Figure 3D. Fan et al. obtained from the calibration model that in the range of a water depth from 0.5 to 10 m, the particle size range was easy to generate free radicals from 42 to 194 μm for air MNBs, and 127 to 470 μm for oxygen MNBs [116].

(4) Temperature: The temperature also has a role in ⁻OH generation by MNBs. Yu et al. explained that in an alkaline MNB solution, the ROS concentration first increased and then decreased with the temperature rise [110]. By this effect, a parabolic trend was shown, where the ROS concentration reached its maximum at 65 °C (Figure 3E). They attributed this phenomenon to the combined effect of the temperature on the oxygen reactivity, diffusion coefficient, and dissolved oxygen concentration (where ROS and ·OH change in the same trend). Wang et al. described the effect of the temperature on the degradation of rhodamine B by cavitation-induced and rotating jets [117]. The results showed that the degradation efficiency of rhodamine B increased when the temperature increased from 20 °C to 40 °C, and decreased when the temperature further increased from 40 °C to 60 °C.

Correspondingly, Wang et al. studied the effect of temperature on the degradation of alachlor by hydrodynamic cavitation [118], finding that the degradation rate of alachlor increased when the temperature increased from 30 °C to 40 °C. However, it decreased when the temperature reached from 40 °C to 60 °C. These findings also prove that the temperature has a dual effect on the ·OH generation by MNBs. Due to the increase of equilibrium vapor pressure, the rise in temperature promotes the formation of MNBs, which is favorable to the generation of ·OH and the degradation of organic matter. However, if the temperature is too high, water vapor will fill the cavitation bubbles and alleviate the bubble collapse, which is not conducive to the generation of ·OH and degradation of organic matter [119,120]. It is worth noting that the temperature influences other test conditions, which should be comprehensively considered to the actual conditions.

(5) External stimulus: MNBs can generate ·OH, but the number generated does not meet the needs of practical engineering applications. External conditions are also required to promote the generation of ·OH by MNBs, such as ultrasonic stimulation, catalysts addition, ultraviolet irradiation, etc. Thus, the role of these external stimuli in the process of ·OH generation by MNBs cannot be ignored. It has been noticed that ultrasonic cavitation is one of the methods to generate MNBs, and diverse ultrasonic frequencies play a crucial role in the ·OH generation by MNBs. Masuda et al. described the effect of ultrasound frequency on ·OH generation by MNBs [121]. The results showed that an ultrasound at 45 kHz promoted ·OH generation in an MNB solution, while an ultrasound at 28 kHz and 100 kHz inhibited ·OH generation. This may be influenced by the ultrasound at 45 kHz that interacts with MNBs with a diameter of about 1 μm and forms new diminutive cavitation bubbles; hence, it is suitable for ⁻OH generation [122]. MBs interfered with the standing wave sound field established by the ultrasonic transducer and reduced the hot spot generated by the cavitation bubble collapse. This indicated that frequencies of 28 kHz and 100 kHz ultrasound were not conducive to ·OH generation [122]. The influence mechanism of ultrasonic frequency on the generation of ·OH by MNBs remains to be further analyzed. Various investigations have shown that the content of ·OH generated by MNBs is proportional to the ultrasonic time and power under a condition of less than 225 w [123]. Through electron spin resonance spectroscopy, it was found that copper as a catalyst could significantly enhance the ·OH generated by the collapse of oxygen or air MNBs under acidic conditions. This may be related to the environmental changes inside the ruptured MBs [111]. Tasaki et al. studied the degradation of methyl orange by MNBs under the irradiation of a low-pressure mercury lamp, indicating that ultraviolet irradiation with a wavelength of 185 nm promoted the generation of ·OH by MNBs and improved the decolorization efficiency of methyl orange [124]. Gao et al. used a fluorescent probe method to determine the ·OH concentration, and found that under ultraviolet irradiation, the content of ·OH generated by ozone MNBs increased by 2–6 times [125].

Based on the above, it was noticed that the generation of ⁻OH by MNBs can be more or less affected by various internal or external factors. And the pH and external stimuli have more influence on ·OH generation in situ than other factors. To make MNBW generate a high concentration of ·OH as much as possible, under the conditions of selecting a favorable air source (oxygen or ozone), maintaining a better pH and temperature, and controlling the bubble size within a certain range, the generation of ·OH can be further enhanced using ultrasonic stimulation, ultraviolet irradiation, or the addition of catalysts.

4. Effect of MNB Mechanism on Pollutants and Biofilms in Water

4.1. MNBs Remove Pollutants from Water

Due to the superior characteristics of MNBs, a broad application value in pollutant removal from water has been developed. On the one hand, MNBs have a strong adsorption capacity and can adsorb pollutants at the MNBs interface; additionally, the collapse of MNBs generates ·OH, which can effectively oxidize and degrade pollutants. And at the same time of bubble collapse, it also has a certain impact on the pollutants, which intensifies the removal efficiency. In addition, MNBs have a high mass transfer efficiency that can

increase the level of dissolved oxygen in water, which improves the microbial activity and contributes to the biodegradation of pollutants. Therefore, MNB technology is widely used to remove pollutants from water.

Lu et al. confirmed the application of MNB coagulation technology in drinking water treatment [126], reporting that the MNB coagulation process could significantly improve the humic acid removal efficiency (DOC removal efficiency increased by 27.9%), which had potent practical application potential in drinking water treatment. Hu and Xia studied ozone MNB applications to repair groundwater contaminated by organic matter and evaluated field tests on trichloroethylene-contaminated sites, showing that the total removal rate of trichloroethylene reached 99% after six days of treatment [53]. Xia and Hu. conducted an experiment using ozone MNBs to treat groundwater containing complex persistent organic pollutants [127], showing that after 30 min of treatment, most benzene and chlorobenzene molecules were effectively removed, with a removal efficiency of more than 95%. Moreover, they used ozone MNBs to degrade methyl orange in surface water and groundwater, which achieved a remarkable treatment effect [128]. Achar et al. reported the removal effect of ozone MNBs on butylated hydroxytoluene, and the result showed that compared with the traditional ozone-based process, ozone MNBs could effectively degrade butylated hydroxytoluene and reduce its toxicity, in which ·OH played a key role [129]. Li et al. used MNBs to degrade phenol and found that the removal rate of phenol by oxygen MBs reached 83% after two hours of treatment [114]. MNBs can also effectively degrade a variety of organic pollutants, and the degradation of organic matter follows pseudo-first-order kinetics, as we can see in Table 6.

Table 6. Organic pollutants degraded by MNBs.

Pollutants	Generation of MNBs	Type of Air Source	Reaction Time (min)	Initial Concentration/(mg/L)	pH	Temperature	Degradation Rate Constant/Degradation Rate/lnc/c$_0$	References
Alachlor	Swirling jet-induced cavitation	Air	100	50	5.9	40 °C	4.90×10^{-2} min^{-1}	[118]
Rhodamine B	Swirling jet-induced cavitation	Air	180	5	5.4	40 °C	62%/5.13×10^{-3} min^{-1}	[117]
Diethyl phthalate	Aeration method	O$_3$	30	222	9	25 °C	98%	[130]
Phenol	Dissolved gas release method	O$_2$	120	18.8	2.3	35 °C	83%/2.67×10^{-2} min^{-1}	[114]
	Dissolved gas release method	Air	180	/	<7	<50 °C	30%	[91]
	Micro bubble ozonation reactor	O$_3$ + Ga(OH)$_2$	40	450	/	25 °C	99%	[131]
Methyl orange	Spiral liquid flow-coupled pressurized dissolution	O$_3$	30	10	/	20 °C	96%	[128]
	Aeration method	O$_3$	30	50	3~11	20 °C	>90%	[127]
	Spiral liquid flow-type	O$_3$	30	10	/	/	98%	[53]
Photoresist	Dissolved gas release method	O$_3$	9.6	/	/	22 °C	100%	[92]
Butylated hydroxytoluene	Aeration method	O$_3$	0.5	<2	7	/	97%	[129]
Dimethyl sulfoxide	Aeration method	O$_3$	/	/	/	/	$7.0 \times 10^{-4} - 1.9 \times 10^{-3}$ s^{-1}	[132]
P-chlorophenol	Ultrasonic cavitation	Air	120	/	/	38 °C	0.00899 min^{-1}/−0.83	[133]
P-nitrophenol	Jet cavitation reactor	Air	90	8	3.5	/	50%	[134]
Trichloroethylene	Aeration method	O$_3$	20	14	/	/	100%	[135]
Polyvinyl alcohol	Dissolved gas release method	O$_3$	120	/	<7	<35 °C	30%	[112]
Benzothiophene	Ultrasonic cavitation	Air	60	/	5	25 °C	0.0492 min^{-1}	[136]

Notably, the degradation of organic pollutants by MNBs has a certain relationship with the pH. The investigation results show that the acid condition is effective in the degradation of the pollutants by MNBs; on the contrary, other research results show that the alkaline environment is suitable for the degradation of pollutants by MNBs. For instance, methyl orange [127], phenol [114], and rhodamine B [117] were best degraded by MNBs under acidic conditions. Nevertheless, the alachlor [118], benzothiophene (BT) [136], and diethyl phthalate [130] degradation by MNBs were successful under alkaline conditions (Figure 4). This is because the pH affects the free radicals generated by MNBs and the physical and chemical properties of the pollutant itself. Therefore, the degradation of organic pollutants by MNBs indicates the dual action of the above two aspects, and we should take this into comprehensive consideration.
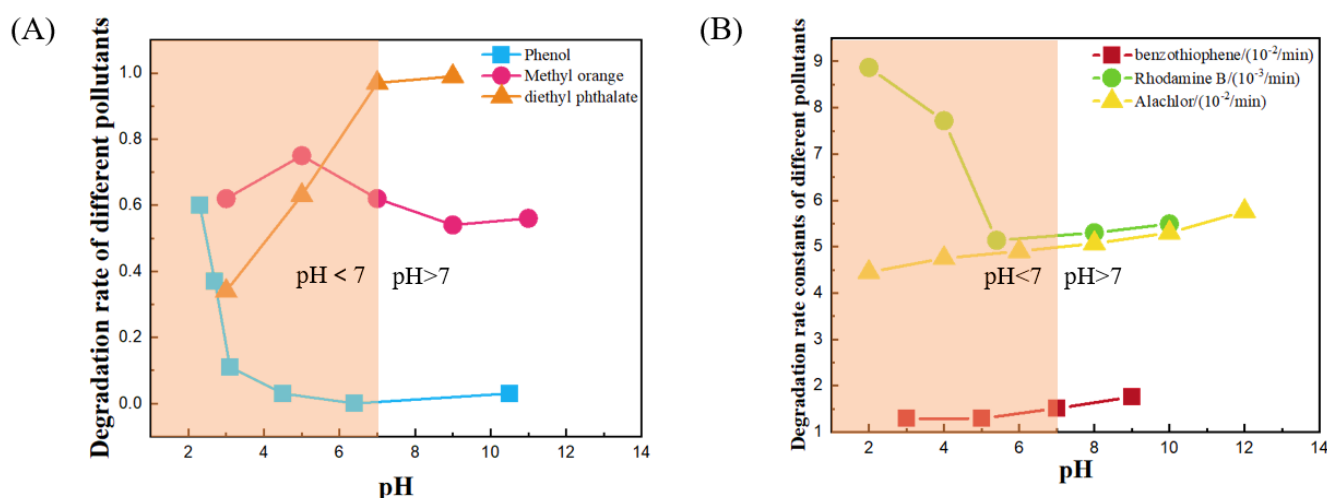
Figure 4. Effect of pH on the degradation of organic pollutants by MNBs. (**A**) Degradation rates of different pollutants by MNBs. (**B**) Degradation rate constants of different pollutants by MNBs. (Ref. [117], reproduced with permission from [Wang Xikui et al.], [Ultrasonics sonochemistry]; published by [ELSEVIER], [2008]; Ref. [118], reproduced with permission from [Wang Xikui and Zhang Yong], [Journal of hazardous materials]; published by [Elsevier], [2009]; Ref. [127], reproduced with permission from [Xia Zhiran and Hu Liming], [Water]; published by [MDPI], [2018]; Ref. [130], reproduced with permission from [Abdisa Jabesa and Pallab Ghosh], [Journal of Environmental Management]; published by [ELSEVIER], [2016]; Ref. [132], reproduced with permission from [Li Pan et al.], [Industrial & engineering chemistry research]; published by [ACS], [2009]; Ref. [136], reproduced with permission from [Il-Kyu Kim and Chin-Pao Huang], [Journal of the Chinese Institute of Engineers]; published by [Springer Nature Singapore Pte Ltd.], [2005]).

4.2. Control Mechanism of MNBs on Pipe Biofilm Growth

The existence of microorganisms seriously affects the water quality safety in pipelines and threatens human health. A wide use of traditional disinfection methods has unsatisfactory effects on biofilm control and produces disinfection by-products, inducing secondary pollution. In recent years, as a clean, safe, and efficient disinfection method, MNB technology has shown great potential in alleviating biofilms by generating decisive oxidative ·OH in situ. As seen in Figure 5, MNBs can inhibit biofilms from physical, chemical, and thermal effects. In terms of physical results, the micromotor drive test [101] and cavitation erosion phenomenon [137] indicate that MNBs induce microjet, shock wave, and shear stresses in the surrounding liquid during collapse and release a large amount of energy. Based on these effects, they break microorganism cell membranes/cell walls and drive the microbial attachment site to move, disrupting the biofilm and causing it to fall off. For the chemical effects, firstly, ·OH can degrade organic matter in water, reduce the food source of microorganisms, and inhibit the metabolism and activity of microorganisms. Secondly, ·OH can directly kill microorganisms in water and reduce the total amount of microorganisms

(the mechanism of ·OH-inactivating microorganisms can be attributed to two aspects [138]: i. oxidation and destruction of the cell wall and membrane of microorganisms and ii. ·OH diffusion into the cell interior inactivates enzymes, damages intracellular components, interferes with protein synthesis and DNA structure, etc.). For thermal effects, the local high temperature generated by the surrounding liquid when MNBs collapse promotes the thermal inactivation of microorganisms. Therefore, MNBs can inhibit biofilm formation from physical, chemical, and thermal effects, and their damage to microorganisms combines the above three result types (Figure 5) [108,139].
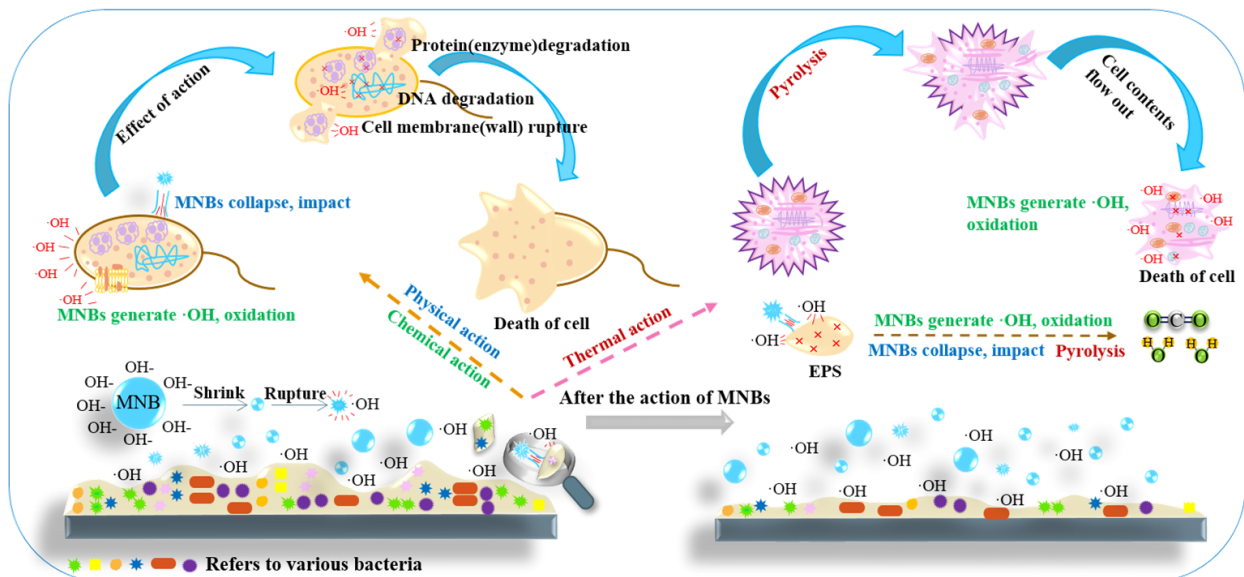
Figure 5. Control mechanism of physical, chemical, and thermal effects of MNBs on biofilm.

Physically, microflows generated by stable cavitation have been shown to have stresses sufficient to destroy cell membranes [139] and are widely used to destroy microbial cells to obtain intracellular derivatives. Based on the mechanism of microbial cell destruction in high-speed and high-pressure homogeneous reactors, it was found that cavitation collapse and the resulting pressure pulse played a crucial role in the cell destruction process [140]. Mason et al. explained that the shear stress and liquid jet generated by the collapse of MNBs might cause physical damage to the cell walls/membranes of microorganisms, and the jet might cause significant pressure on the microbial species, thus contributing to sterilization [141]. Chemically, some studies have reported the application of MNBs in the physical–chemical–biological composite fouling of plugging irrigator. Tan et al. examined the alleviating effect of NBs on the composite clogging of the irrigator of the biogas slurry dripper system [142]. The results indicated that the EPS content in dirt under the NB treatment was significantly reduced by 29%–53% compared with the control group. The experimental results were consistent with the research results [143], which showed that the mass of EPS in the irrigator was reduced by 29%–53% under the treatment of oxygen MNBs. The investigation described that MNB aeration diminished the diversity and richness of the microbial community in the adhesive blockage of the irrigator and reduced the number of core bacteria that affected the blockage of the irrigator [123]. Guo et al. reported that the strong oxidizing ·OH generated by NBs during the collapse process played an essential role in the microorganisms' removal in water [46]. MNB technology is widely applied in controlling membrane pollution, which can reduce the occurrence of membrane pollution by reducing the EPS content. Agarwal et al. found that NB treatment could effectively alleviate membrane pollution caused by biofilm attachment [144]. In addition, the ·OH generated by MNBs is used in water disinfection treatment, which can effectively remove bacteria, yeast, and viruses in water [145]. Thermally, the study showed that the collapse of oxygen NBs might induce the liquid temperature at the bubble wall to rise to 94 °C,

and the collapse of air NBs might induce the liquid temperature at the bubble wall to rise to 85 °C [82]. Sun et al. employed the new hydrodynamic cavitation reactor to generate MNBs for disinfection [108]. Within 14 min, the collapse of MNBs induced the surrounding water temperature to rise to 65.7 °C and achieved the 100% removal of *Escherichia coli* in water samples.

5. Application Prospect of MNBs in Drinking Water

Human beings need to consume 2–3 liters (L) of drinking water every day, and the quality of drinking water is crucial to human health. Ensuring the safety of drinking water quality is the premise and basis for improving human health and people's well-being. Drinking water quality safety mainly involves two aspects: chemical safety and biological safety. The existence of various organic pollutants and pathogenic microorganisms in drinking water brings potential risks to human health and reduces the chemical and biological safety of drinking water. Therefore, the problem of drinking water quality safety mainly relies on the removal of organic matter and microorganisms in water. Traditional drinking water treatment technologies often depend on catalysts and chemical reagents, leading to secondary pollution along the purifying water. Nevertheless, the emerging MNB technology generates potent oxidizing ·OH in the process of bubble collapse, which is green and clean, having great potential in improving the chemical and biological characteristics of drinking water, being safe and efficient. The application prospects of MNBs in drinking water are shown in Figure 6.
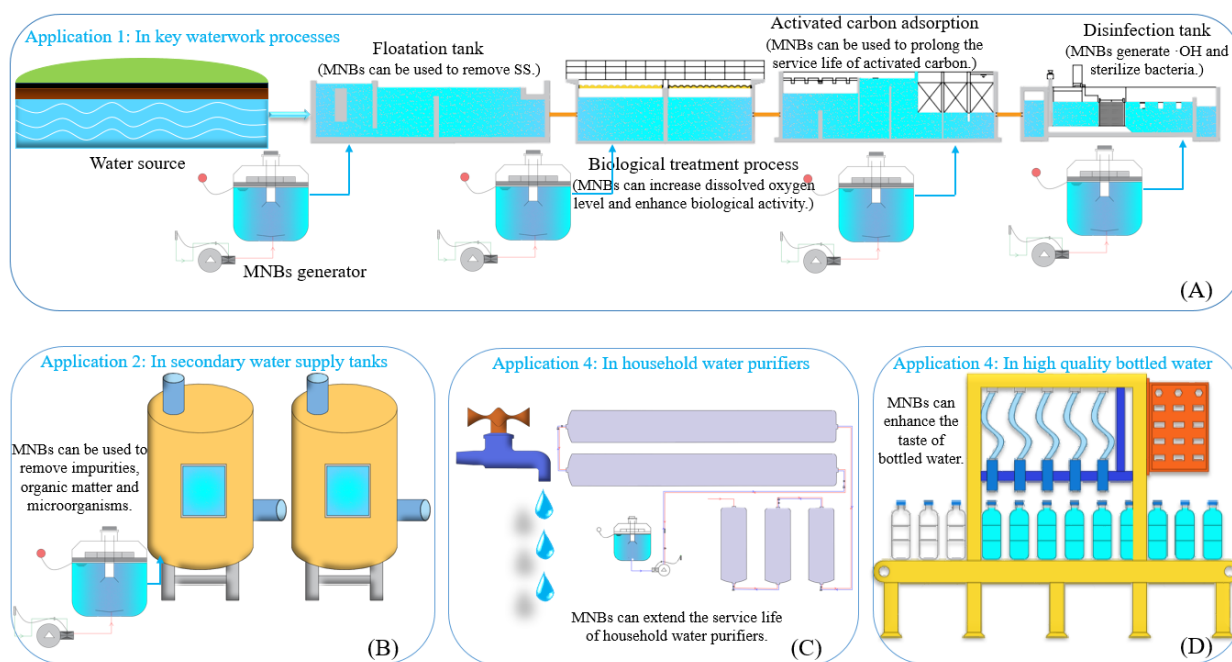

Figure 6. Application prospects of MNBs in drinking water. (**A**) Application of MNBs in waterwork processes. (**B**) Application of MNBs in second water supply tanks. (**C**) Application of MNBs in household water purifiers. (**D**) Application of MNBs in high quality bottled water.

(1) Removal of organic matter from drinking water: A drinking water system includes the source water, waterworks, water supply pipeline network, and tap water, etc. Surface water (i.e., rivers, reservoirs, and lakes) and groundwater are vital drinking water sources; hence, ensuring their safety and cleanliness is highly required. With the aggravation of environmental pollution, a variety of emerging pollutants and refractory organic compounds (e.g., persistent organic contaminants, endocrine disrupters, pharmaceuticals, personal care products, and microplastics) have seriously contaminated the drinking water system and triggered harm to the drinking water safety and human health. Compared

with conventional pollutants, these emerging pollutants have the characteristics of a low concentration (ng/L–µg/L), difficult biodegradation, easy migration and transformation, easy bioenrichment, high toxicity, and long life. These characteristics make their control and removal a prominent challenge in the environment. Over recent years, advanced oxidation technologies based on ·OH have been widely used in various organic pollutants reduction, but they usually need to add chemicals or consume energy to generate ·OH, which has certain limitations. On the one hand, drinking water has very high requirements in regard to the water quality, which is sensitive, and traditional water purification methods may pose specific threats to the drinking water quality; on the other hand, compared with other water purification methods, MNBs generate ·OH during its collapse process, which is green and clean and does not produce any secondary pollution. Therefore, MNB technology is very suitable for use in drinking water. Moreover, we described in Part 3.1 that the practical application of MNBs in water sources with a more complex water quality than drinking water indicates a potential application prospect in drinking water treatment. The use of MNB technology to remove emerging pollutants and refractory organic matter in drinking water is bound to become a very effective method and means.

(2) Remove biofilms from water supply pipeline network: In drinking water distribution systems, microorganisms can be present in bulk water (such as planktonic bacteria) or attached to pipes (such as biofilms or loose sediments) [146], where the biomass present in biofilms accounts for about 95% [146,147]. In contrast with the microorganisms in the bulk water, the microorganisms in the biofilm have a higher density and biological activity, which is more difficult to inactivate, causes pipe corrosion, and directly brings a variety of water-borne diseases (e.g., cholera, diarrhea, dysentery, and polio). Therefore, ensuring the biosafety of drinking water is mainly about reducing biofilm growth in the water supply pipeline. As mentioned in Part 3.2, MNBs can remove microorganisms from three aspects: thermal, physical, and chemical effects, and MNB technology is widely applied in microbial cell destruction, the control of physical–chemical–biological composite fouling, membrane biological contamination, disinfection, and sterilization, both in terms of experimental phenomena and mechanisms. Based on the experimental phenomena and mechanisms, MNBs have shown a promising alternative to control biofilms. Based on this, MNBs technology is expected to be a reliable method to control the biofilm formation of water supply network, inducing a capable application prospect in the water supply pipeline network biofilm control.

(3) Application of MNBs in practical engineering: MNBs can generate ·OH and shear stress to degrade pollutants and sterilize bacteria. Consequently, MNB technology can be applied to water sources to remove organic pollutants and microorganisms. In waterworks process, for instance, MNBs are used in the floatation tank to remove SS due to their strong adsorption ability, in the biological treatment process to improve the DO level and biological activity of the water due to their high mass transfer efficiency, and in the disinfection tank to kill microorganisms due to their ·OH generation characteristic. They can be used in a secondary water supply tank to inhibit the growth of biofilms in the tank, remove the rust impurities, and remove organic pollutants mixed in the process of water flow in the pipeline. They can be used in household water purifiers to ensure water quality safety and extend the service life of a filter element, as shown in Figure 6. Moreover, this paper focuses on applying this technology to bottled water preparation for the first time. Under the condition of safety, 15 young people aged 20 to 30 years old were asked to taste water. It was found that compared with ordinary drinking water, 85.7% of people thought that MNB water was soft or softer, and 73.3% of people thought that MNB water was sweet or sweeter. For that reason, MNB technology can be applied to the bottled water production line to produce high quality bottled water containing MNBs, as shown in Figure 7. In terms of the impact of MNBs on human health, McEwan et al. used oxygen MNBs to deliver oxygen to the vicinity of the tumor, enhancing the sonodynamic therapy of hypoxic tumors. Subsequently, in combination with sonodynamic and antimetabolite therapy, they used oxygen MNBs as delivery carriers to improve the treatment of pancreatic cancer [148,149].

From the application of MNB technology in medicine, it is inferred that MNBs are harmless to human health, and more research is still needed in the future to further explore the impact. To sum up, MNB technology has a very broad prospect in drinking water, and we should shift the research purpose to the application of MNB technology in drinking water.
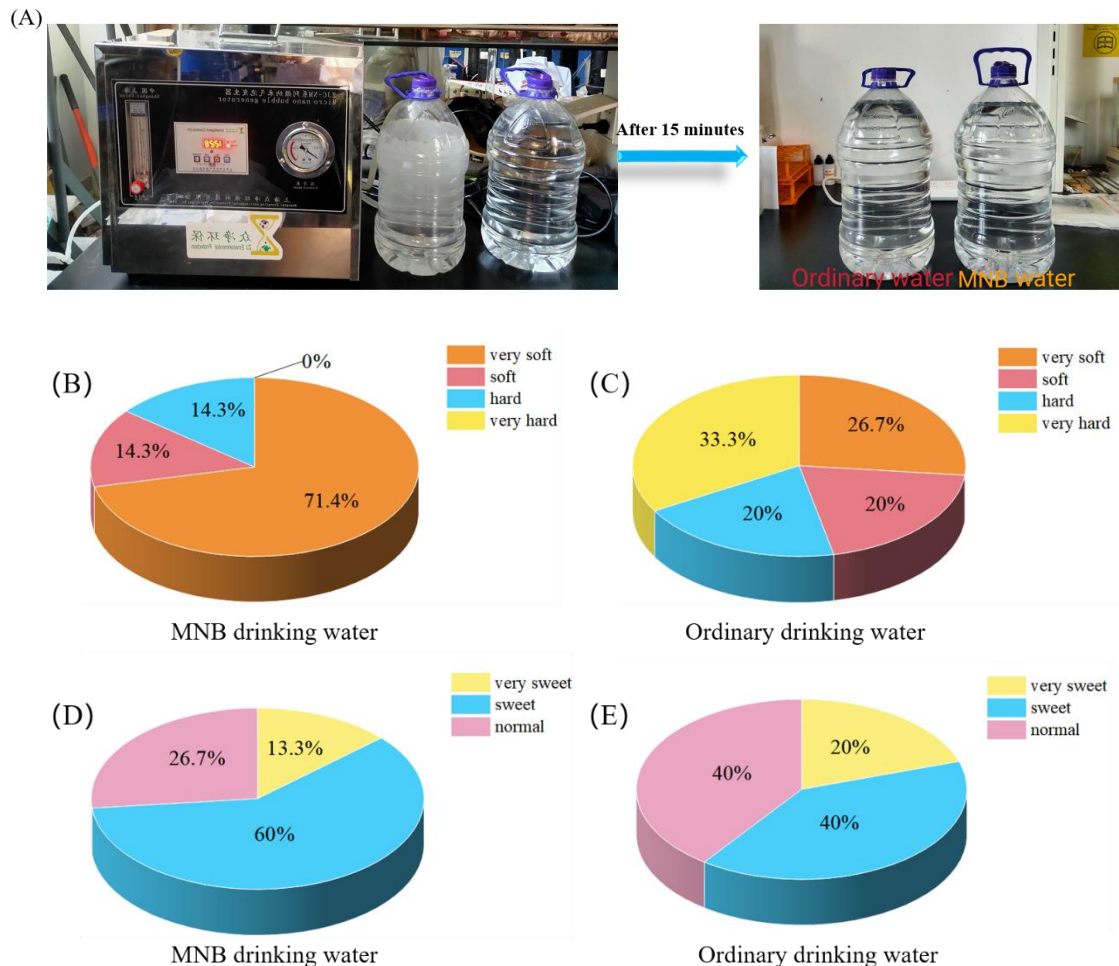

Figure 7. Survey results of MNB drinking water and ordinary drinking water. (**A**) MNB drinking water and ordinary drinking water. (**B**) Investigation results of hardness of MNB drinking water. (**C**) Investigation results of hardness of ordinary drinking water. (**D**) Investigation result of sweetness of MNB drinking water. (**E**) Investigation results of sweetness of ordinary drinking water.

6. Limitations and Prospects of MNBs

Although MNB technology has been applied in various fields, the MNB investigation has not been deeply explored yet; therefore, there are still blind spots that require our attention. As an example of possible gaps found in this study, they are described as follows:

1. The long-term stable existence of MNBs in water and the ·OH generation mechanism are highly controversial. Existing studies on the above two aspects remain at the surface and speculation level; hence, further discussion is needed.
2. The relationship between the synergistic and antagonistic effects of MNBs on microorganisms remains unclear, because the MNBs can generate substantial oxidizing ·OH to destroy microorganisms and provide great potential for water disinfection. Moreover, due to a high mass transfer efficiency, MNBs have a good biological activity and can promote the biological purification function of water. These two statements are contradictory. Therefore, to effectively apply MNB technology, it is essential to investigate the circumstances under which either the synergistic or antagonistic effects of MNBs on microorganisms prevail.

3. It is difficult to quantitatively determine the $\cdot$OH generated by MNBs. Recently, the detection methods of $\cdot$OH are all indirect methods, which are complicated in operation, and are inevitably interfered by many factors in the detection process, resulting in considerable errors. Future research should focus on the direct detection of $\cdot$OH to reduce unnecessary interference items.

4. MNBs generate a limited number of $\cdot$OH. The ability of MNBs to generate free radicals is only one of its many outstanding properties, and the $\cdot$OH generated is only one of the many free radical products. At present, studies on the influence of various factors on the generation of $\cdot$OH by MNBs are relatively simple. They should continue to explore how to promote the generation of $\cdot$OH by MNBs and simultaneously control the factors that affect $\cdot$OH generation under optimal conditions.

5. NB generation devices are expensive. NBs are superior to MBs in all aspects, but due to the high energy consumption and high price of NB generation devices, the application of NBs in various fields is limited to a certain extent. Hence, developing practical NB generation devices with a low energy consumption, low cost, excellent performance, and easy promotion is also a new potential direction of current research.

6. The study of MNB characteristics is not comprehensive enough. At present, the research on the characteristics of MNBs mainly focuses on the well-known aspects of free radical generation and high mass transfer efficiency. Other characteristics of MNBs, such as heat transfer and viscosity, are unknown and require more analysis.

Although the current research on MNBs is not mature, the outstanding characteristics of MNBs have gradually applied and promoted in various fields. In particular, in the environmental domain, it plays a crucial role in the drinking water treatment application. It is assumed that with additional research on MNBs, it will become an indispensable technology in engineering applications.

7. Conclusions

This review analyzed ten methods for generating MNBs in water. Whether mechanical or chemical, the size distribution of MNBs generated ranges from tens of nanometers to tens of micrometers, and the size distribution was uneven. In addition, different generation methods are affected by the conditions of the method itself, instrument parameters, etc., so we need to coordinate control to obtain stable MNBW. In contrast, with ordinary bubbles, MNBs have the advantages of good stability, efficient mass transfer ability, and high absolute zeta potential value. We focus on the characteristics that MNBs can generate $\cdot$OH and discuss the influence of various factors on the generation of $\cdot$OH. Among them, the pH and type of gas source affect the kind of free radicals and the number of $\cdot$OH generated by MNBs. The bubble size and temperature affect the number of $\cdot$OH generated by MNBs, and the number of $\cdot$OH varies with the two factors in a parabolic shape. Ultrasonic, ultraviolet, and catalyst methods can be used to promote the $\cdot$OH generation by MNBs. However, no consensus has been reached on the mechanism of the generation of $\cdot$OH by MNBs.

There are two main theories (i.e., ion accumulation theory and adiabatic compression theory), which mention that the high absolute zeta potential value at the MNB interface plays a crucial role in $\cdot$OH generation and that the high temperature and pressure during the collapse of MNBs induce the $\cdot$OH generation. This review focuses on the application of MNBs in the water treatment field due to their characteristics of $^-$OH generation, shear stress, and microjets generated by the surrounding environment during the collapse. It can be extended to remove pollutants in drinking water and inhibit biofilm formation in the water supply network. It indicates that contrasted to other techniques, MNB technology possesses the advantages of being green, safe, clean, and efficient. Nevertheless, the removal mechanism of MNBs on organic matter and microorganisms is still unclear and has not been deeply analyzed and studied; hence, it requires our attention in the future. In practical projects, MNB technology can be used for secondary water supply tanks and household water purifiers to increase the water quality and extend the service life of the filter element. Based on the survey conducted, compared with ordinary drinking water,

85.7% of people think that MNB drinking water is soft or softer, and 73.3% of people think that MNB water is sweet or sweeter; therefore, MNBs can also be used in bottled water production lines to enhance the taste of drinking water. We expect that in the future, we all can explore more new investigations and potential applications of MNBs in various research fields.

References

1. Mekal, A.D.; El-Shazly, M.M.; Ragab, M.; Marzouk, E.R. Comparison of modern and 40-year-old drinking water pipeline in northern Sinai region, Egypt: Characteristics and health risk assessment. *J. Trace Elem. Miner.* **2023**, *5*, 10078. [CrossRef]
2. Chang, L.; Lee, J.H.W.; Fung, Y.S. Prediction of lead leaching from galvanic corrosion of lead-containing components in copper pipe drinking water supply systems. *J. Hazard. Mater.* **2022**, *436*, 129169. [CrossRef] [PubMed]
3. Liu, J.; Chen, H.; Yao, L.; Wei, Z.; Lou, L.; Shan, Y.; Endalkachew, S.-D.; Mallikarjuna, N.; Hu, B.; Zhou, X. The spatial distribution of pollutants in pipe-scale of large-diameter pipelines in a drinking water distribution system. *J. Hazard. Mater.* **2016**, *317*, 27–35. [CrossRef] [PubMed]
4. Barton, N.A.; Farewell, T.S.; Hallett, S.H.; Acland, T.F. Improving pipe failure predictions: Factors affecting pipe failure in drinking water networks. *Water Res.* **2019**, *164*, 114926. [CrossRef]
5. Kim, J.R.; Huling, S.G.; Kan, E. Effects of temperature on adsorption and oxidative degradation of bisphenol A in an acid-treated iron-amended granular activated carbon. *Chem. Eng. J.* **2015**, *262*, 1260–1267. [CrossRef]
6. Yüksel, S.; Kabay, N.; Yüksel, M. Removal of bisphenol A (BPA) from water by various nanofiltration (NF) and reverse osmosis (RO) membranes. *J. Hazard. Mater.* **2013**, *263*, 307–310. [CrossRef] [PubMed]
7. Zhang, H.; Lin, H.; Li, Q.; Cheng, C.; Shen, H.; Zhang, Z.; Zhang, Z.; Wang, H. Removal of refractory organics in wastewater by coagulation/flocculation with green chlorine-free coagulants. *Sci. Total Environ.* **2021**, *787*, 147654. [CrossRef]
8. Baig, S.; Liechti, P.A. Ozone treatment for biorefractory COD removal. *Water Sci. Technol.* **2001**, *43*, 197–204. [CrossRef] [PubMed]
9. Pera-Titus, M.; García-Molina, V.; Baños, M.A.; Giménez, J.; Esplugas, S. Degradation of chlorophenols by means of advanced oxidation processes: A general review. *Appl. Catal. B Environ.* **2004**, *47*, 219–256. [CrossRef]
10. Brillas, E.; Sirés, I.; Oturan, M.A. Electro-Fenton process and related electrochemical technologies based on Fenton's reaction chemistry. *Chem. Rev.* **2009**, *109*, 6570–6631. [CrossRef]
11. Moreira, F.C.; Garcia-Segura, S.; Vilar, V.J.P.; Boaventura, R.A.; Brillas, E. Decolorization and mineralization of Sunset Yellow FCF azo dye by anodic oxidation, electro-Fenton, UVA photoelectro-Fenton and solar photoelectro-Fenton processes. *Appl. Catal. B Environ.* **2013**, *142*, 877–890. [CrossRef]
12. Subramanian, G.; Prakash, H. Photo augmented copper-based Fenton disinfection under visible LED light and natural sunlight irradiation. *Water Res.* **2021**, *190*, 116719. [CrossRef]
13. Li, T.; Shang, C.; Xiang, Y.; Yin, R.; Pan, Y.; Fan, M.; Yang, X. ClO_2 pre-oxidation changes dissolved organic matter at the molecular level and reduces chloro-organic byproducts and toxicity of water treated by the UV/chlorine process. *Water Res.* **2022**, *216*, 118341. [CrossRef]
14. Xu, M.Y.; Lin, Y.L.; Zhang, T.Y.; Hu, C.Y.; Tang, Y.L.; Deng, J.; Xu, B. Chlorine dioxide-based oxidation processes for water purification: A review. *J. Hazard. Mater.* **2022**, *436*, 129195. [CrossRef] [PubMed]
15. Kurniawan, T.A.; Lo, W.; Chan, G.; Sillanpää, M.E. Biological processes for treatment of landfill leachate. *J. Environ. Monit.* **2010**, *12*, 2032–2047. [CrossRef] [PubMed]

16. Ilmasari, D.; Kamyab, H.; Yuzir, A.; Riyadi, F.A.; Khademi, T.; Al-Qaim, F.F.; Kirpichnikova, I.; Krishnan, S. A Review of the Biological Treatment of Leachate: Available Technologies and Future Requirements for the Circular Economy Implementation. *Biochem. Eng. J.* **2022**, *187*, 108605. [CrossRef]
17. Zhang, T. The development of drinking water treatment technology. *China High-Tech Enterp.* **2013**, *23*, 6–8.
18. Zhai, H.; He, X.; Zhang, Y.; Du, T.; Adeleye, A.S.; Li, Y. Disinfection byproduct formation in drinking water sources: A case study of Yuqiao reservoir. *Chemosphere* **2017**, *181*, 224–231. [CrossRef]
19. Pokhrel, D.; Viraraghavan, T. Biological filtration for removal of arsenic from drinking water. *J. Environ. Manag.* **2009**, *90*, 1956–1961. [CrossRef]
20. Schijven, J.F.; van den Berg, H.H.J.L.; Colin, M.; Dullemont, Y.; Hijnen, W.A.M.; Magic-Knezev, A.; Oorthuizen, W.A.; Wubbels, G. A mathematical model for removal of human pathogenic viruses and bacteria by slow sand filtration under variable operational conditions. *Water Res.* **2013**, *47*, 2592–2602. [CrossRef]
21. Hedegaard, M.J.; Albrechtsen, H.J. Microbial pesticide removal in rapid sand filters for drinking water treatment–potential and kinetics. *Water Res.* **2014**, *48*, 71–81. [CrossRef] [PubMed]
22. Cai, Y.; Li, D.; Liang, Y.; Zeng, H.; Zhang, J. Autotrophic nitrogen removal process in a potable water treatment biofilter that simultaneously removes Mn and NH4+-N. *Bioresour. Technol.* **2014**, *172*, 226–231. [CrossRef]
23. Pramanik, B.K.; Choo, K.-H.; Pramanik, S.K.; Suja, F.; Jegatheesan, V. Comparisons between biological filtration and coagulation processes for the removal of dissolved organic nitrogen and disinfection by-products precursors. *Int. Biodeterior. Biodegrad.* **2015**, *104*, 164–169. [CrossRef]
24. Li, Z.; Dvorak, B.; Li, X. Removing 17β-estradiol from drinking water in a biologically active carbon (BAC) reactor modified from a granular activated carbon (GAC) reactor. *Water Res.* **2012**, *46*, 2828–2836. [CrossRef]
25. Yapsakli, K.; Mertoglu, B.; Çeçen, F. Identification of nitrifiers and nitrification performance in drinking water biological activated carbon (BAC) filtration. *Process Biochem.* **2010**, *45*, 1543–1549. [CrossRef]
26. Zhang, X.X.; Zhang, Z.Y.; Ma, L.P.; Liu, N.; Wu, B.; Zhang, Y.; Li, A.M.; Cheng, S.P. Influences of hydraulic loading rate on SVOC removal and microbial community structure in drinking water treatment biofilters. *J. Hazard. Mater.* **2010**, *178*, 652–657. [CrossRef] [PubMed]
27. McKie, M.J.; Andrews, S.A.; Andrews, R.C. Conventional drinking water treatment and direct biofiltration for the removal of pharmaceuticals and artificial sweeteners: A pilot-scale approach. *Sci. Total Environ.* **2016**, *544*, 10–17. [CrossRef]
28. Akcay, M.U.; Avdan, Z.Y.; Inan, H. Effect of biofiltration process on the control of THMs and HAAs in drinking water. *Desalination Water Treat.* **2016**, *57*, 2546–2554. [CrossRef]
29. Tekerlekopoulou, A.G.; Vayenas, D.V. Ammonia, iron and manganese removal from potable water using trickling filters. *Desalination* **2007**, *210*, 225–235. [CrossRef]
30. Hasan, H.A.; Abdullah, S.R.S.; Kamarudin, S.K.; Kofli, N.T. Response surface methodology for optimization of simultaneous COD, NH4+–N and Mn2+ removal from drinking water by biological aerated filter. *Desalination* **2011**, *275*, 50–61. [CrossRef]
31. Han, M.; Zhao, Z.-W.; Gao, W.; Cui, F.-Y. Study on the factors affecting simultaneous removal of ammonia and manganese by pilot-scale biological aerated filter (BAF) for drinking water pre-treatment. *Bioresour. Technol.* **2013**, *145*, 17–24. [CrossRef] [PubMed]
32. Han, M.; Zhao, Z.; Gao, W.; Tian, Y.; Cui, F. Effective combination of permanganate composite chemicals (PPC) and biological aerated filter (BAF) to pre-treat polluted drinking water source. *Desalination Water Treat.* **2016**, *57*, 28240–28249. [CrossRef]
33. He, S.; Wang, J.; Ye, L.; Zhang, Y.; Yu, J. Removal of diclofenac from surface water by electron beam irradiation combined with a biological aerated filter. *Radiat. Phys. Chem.* **2014**, *105*, 104–108. [CrossRef]
34. Marsidi, N.; Abu Hasan, H.; Abdullah, S.R.S. A review of biological aerated filters for iron and manganese ions removal in water treatment. *J. Water Process Eng.* **2018**, *23*, 1–12. [CrossRef]
35. Buttiglieri, G.; Malpei, F.; Daverio, E.; Melchiori, M.; Nieman, H.; Ligthart, J. Denitrification of drinking water sources by advanced biological treatment using a membrane bioreactor. *Desalination* **2005**, *178*, 211–218. [CrossRef]
36. Li, X.; Chu, H.P. Membrane bioreactor for the drinking water treatment of polluted surface water supplies. *Water Res.* **2003**, *37*, 4781–4791. [CrossRef] [PubMed]
37. Ricardo, A.R.; Carvalho, G.; Velizarov, S.; Crespo, J.G.; Reis, M.A. Kinetics of nitrate and perchlorate removal and biofilm stratification in an ion exchange membrane bioreactor. *Water Res.* **2012**, *46*, 4556–4568. [CrossRef] [PubMed]
38. Matos, C.T.; Velizarov, S.; Reis, M.A.M.; Crespo, J.G. Removal of bromate from drinking water using the ion exchange membrane bioreactor concept. *Environ. Sci. Technol.* **2008**, *42*, 7702–7708. [CrossRef] [PubMed]
39. Xie, S.G.; Wen, D.H.; Shi, D.W.; Tang, X.Y. Reduction of precursors of chlorination by-products in drinking water using fluidized-bed biofilm reactor at low temperature. *Biomed. Environ. Sci.* **2006**, *19*, 360.
40. Tian, J.-Y.; Liang, H.; Li, X.; You, S.-J.; Tian, S.; Li, G.-B. Membrane coagulation bioreactor (MCBR) for drinking water treatment. *Water Res.* **2008**, *42*, 3910–3920. [CrossRef]
41. Tian, J.-Y.; Chen, Z.-L.; Yang, Y.-L.; Liang, H.; Nan, J.; Wang, Z.-Z.; Li, G.-B. Hybrid process of BAC and sMBR for treating polluted raw water. *Bioresour. Technol.* **2009**, *100*, 6243–6249. [CrossRef] [PubMed]
42. Haris, S.; Qiu, X.; Klammler, H.; Mohamed, M.M. The use of micro-nano bubbles in groundwater remediation: A comprehensive review. *Groundw. Sustain. Dev.* **2020**, *11*, 100463. [CrossRef]

43. Sakr, M.; Mohamed, M.M.; Maraqa, M.A.; Hamouda, M.A.; Hassan, A.A.; Ali, J.; Jung, J. A critical review of the recent developments in micro–nano bubbles applications for domestic and industrial wastewater treatment. *Alex. Eng. J.* **2022**, *61*, 6591–6612. [CrossRef]

44. Tan, K.A.; Mohan, Y.; Liew, K.J.; Chong, S.H.; Poh, P.E. Development of an effective cleaning method for metallic parts using microbubbles. *J. Clean. Prod.* **2020**, *261*, 121076. [CrossRef]

45. Xiao, W.; Xu, G.; Li, G. Effect of nanobubble application on performance and structural characteristics of microbial aggregates. *Sci. Total Environ.* **2021**, *765*, 142725. [CrossRef] [PubMed]

46. Guo, Z.; Wang, X.; Wang, H.; Hu, B.; Lei, Z.; Kobayashi, M.; Adachi, Y.; Shimizu, K.; Zhang, Z. Effects of nanobubble water on the growth of Lactobacillus acidophilus 1028 and its lactic acid production. *RSC Adv.* **2019**, *9*, 30760–30767. [CrossRef] [PubMed]

47. Wang, W.; Fan, W.; Huo, M.; Zhao, H.; Lu, Y. Hydroxyl radical generation and contaminant removal from water by the collapse of microbubbles under different hydrochemical conditions. *Water Air Soil Pollut.* **2018**, *229*, 86. [CrossRef]

48. Mezule, L.; Tsyfansky, S.; Yakushevich, V.; Juhna, T. A simple technique for water disinfection with hydrodynamic cavitation: Effect on survival of *Escherichia coli*. *Desalination* **2009**, *248*, 152–159. [CrossRef]

49. Zhu, J.; Wakisaka, M. Effect of air nanobubble water on the growth and metabolism of *Haematococcus lacustris* and *Botryococcus braunii*. *J. Nutr. Sci. Vitaminol.* **2019**, *65*, S212–S216. [CrossRef]

50. Choi, S.J.; Kim, Y.H.; Jung, I.H.; Lee, J.H. Effect of Nano Bubble Oxygen and Hydrogen Water on Microalgae. *Appl. Chem. Eng.* **2014**, *25*, 324–329. [CrossRef]

51. Xiao, W.; Xu, G. Mass transfer of nanobubble aeration and its effect on biofilm growth: Microbial activity and structural properties. *Sci. Total Environ.* **2020**, *703*, 134976. [CrossRef] [PubMed]

52. Hanotu, J.; Kong, D.; Zimmerman, W.B. Intensification of yeast production with microbubbles. *Food Bioprod. Process.* **2016**, *100*, 424–431. [CrossRef]

53. Hu, L.; Xia, Z. Application of ozone micro-nano-bubbles to groundwater remediation. *J. Hazard. Mater.* **2018**, *342*, 446–453. [CrossRef]

54. Wu, Z.; Zhang, X.; Zhang, X.; Li, G.; Sun, J.; Zhang, Y.; Li, M.; Hu, J. Nanobubbles influence on BSA adsorption on mica surface. *Surf. Interface Anal. Int. J. Devoted Dev. Appl. Tech. Anal. Surf. Interfaces Thin Film.* **2006**, *38*, 990–995. [CrossRef]

55. Wu, Z.; Zhang, X.; Zhang, X.; Sun, J.; Dong, Y.; Hu, J. In situ AFM observation of BSA adsorption on HOPG with nanobubble. *Chin. Sci. Bull.* **2007**, *52*, 1913–1919. [CrossRef]

56. Liu, C.; Tang, Y. Application research of micro and nano bubbles in water pollution control. *E3S Web Conf. EDP Sci.* **2019**, *136*, 06028. [CrossRef]

57. Nakashima, T.; Kobayashi, Y.; Hirata, Y. Method to exterminate blue-green algae in a large pond and to improve plant growth by micro-nano bubbles in activated water. In Proceedings of the XXVIII International Horticultural Congress on Science and Horticulture for People (IHC2010): International Symposium on 938, Lisbon, Portugal, 22 August 2010; pp. 391–400.

58. Minamikawa, K.; Takahashi, M.; Makino, T.; Tago, K.; Hayatsu, M. Irrigation with oxygen-nanobubble water can reduce methane emission and arsenic dissolution in a flooded rice paddy. *Environ. Res. Lett.* **2015**, *10*, 084012. [CrossRef]

59. Baram, S.; Weinstein, M.; Evans, J.F.; Berezkin, A.; Sade, Y.; Ben-Hur, M.; Bernstein, N.; Mamane, H. Drip irrigation with nanobubble oxygenated treated wastewater improves soil aeration. *Sci. Hortic.* **2022**, *291*, 110550. [CrossRef]

60. Ebina, K.; Shi, K.; Hirao, M.; Hashimoto, J.; Kawato, Y.; Kaneshiro, S.; Morimoto, T.; Koizumi, K.; Yoshikawa, H. Oxygen and air nanobubble water solution promote the growth of plants, fishes, and mice. *PLoS ONE* **2013**, *8*, e65339. [CrossRef]

61. Li, H.; Hu, L.; Song, D.; Lin, F. Characteristics of micro-nano bubbles and potential application in groundwater bioremediation. *Water Environ. Res.* **2014**, *86*, 844–851. [CrossRef]

62. Sumikura, M.; Hidaka, M.; Murakami, H.; Nobutomo, Y.; Murakami, T. Ozone micro-bubble disinfection method for wastewater reuse system. *Water Sci. Technol.* **2007**, *56*, 53–61. [CrossRef] [PubMed]

63. Liu, S.; Wang, Q.; Ma, H.; Huang, P.; Li, J.; Kikuchi, T. Effect of micro-bubbles on coagulation flotation process of dyeing wastewater. *Sep. Purif. Technol.* **2010**, *71*, 337–346. [CrossRef]

64. Priyadarshini, M.; Das, I.; Ghangrekar, M.M.; Blaney, L. Advanced oxidation processes: Performance, advantages, and scale-up of emerging technologies. *J. Environ. Manag.* **2022**, *316*, 115295. [CrossRef] [PubMed]

65. Temesgen, T.; Bui, T.T.; Han, M.; Kim, T.-I.; Park, H. Micro and nanobubble technologies as a new horizon for water-treatment techniques: A review. *Adv. Colloid Interface Sci.* **2017**, *246*, 40–51. [CrossRef]

66. Huang, C.H. Preparation of Nanobubbles by Ultrasonic Method and Its Effect on Electric Double Layer on Electrode Surface. Master's Thesis, Shanghai Normal University, Shanghai, China, 2016.

67. Maeda, Y.; Hosokawa, S.; Baba, Y.; Tomiyama, A.; Ito, Y. Generation mechanism of micro-bubbles in a pressurized dissolution method. *Exp. Therm. Fluid Sci.* **2015**, *60*, 201–207. [CrossRef]

68. Etchepare, R.; Azevedo, A.; Calgaroto, S.; Rubio, J. Removal of ferric hydroxide by flotation with micro and nanobubbles. *Sep. Purif. Technol.* **2017**, *184*, 347–353. [CrossRef]

69. Huang, Q.; Liu, A.R.; Zhang, L.J. Characteristics of micro-nanobubbles and their applications in soil environment improvement. *J. Environ. Eng. Technol.* **2022**, *12*, 1324–1332.

70. Wu, M.; Song, H.; Liang, X.; Huang, N.; Li, X. Generation of micro-nano bubbles by self-developed swirl-type micro-nano bubble generator. *Chem. Eng. Process.-Process Intensif.* **2022**, *181*, 109136. [CrossRef]

71. Li, J.; Song, Y.; Yin, J.; Wang, D. Investigation on the effect of geometrical parameters on the performance of a venturi type bubble generator. *Nucl. Eng. Des.* **2017**, *325*, 90–96. [CrossRef]

72. Zhao, L.; Sun, L.; Mo, Z.; Du, M.; Huang, J.; Bao, J.; Tang, J.; Xie, G. Effects of the divergent angle on bubble transportation in a rectangular Venturi channel and its performance in producing fine bubbles. *Int. J. Multiph. Flow* **2019**, *114*, 192–206. [CrossRef]

73. Takahashi, M.; Kawamura, T.; Yamamoto, Y.; Ohnari, H.; Himuro, S.; Shakutsui, H. Effect of shrinking microbubble on gas hydrate formation. *J. Phys. Chem. B* **2003**, *107*, 2171–2173. [CrossRef]

74. Azevedo, A.; Etchepare, R.; Calgaroto, S.; Rubio, J. Aqueous dispersions of nanobubbles: Generation, properties and features. *Miner. Eng.* **2016**, *94*, 29–37. [CrossRef]

75. Seddon, J.R.T.; Lohse, D.; Ducker, W.A.; Craig, V.S.J. A deliberation on nanobubbles at surfaces and in bulk. *ChemPhysChem* **2012**, *13*, 2179–2187. [CrossRef] [PubMed]

76. Qiu, J.; Zou, Z.; Wang, S.; Wang, X.; Wang, L.; Dong, Y.; Zhao, H.; Zhang, L.; Hu, J. Formation and stability of bulk nanobubbles generated by ethanol–water exchange. *ChemPhysChem* **2017**, *18*, 1345–1350. [CrossRef] [PubMed]

77. Zhang, L.J.; Chen, H.; Li, Z.X.; Fang, H.P.; Hu, J. The longevity of nanobubbles stems from their high internal density. *Sci. Sin. G Ser.* **2007**, *37*, 556–560.

78. Zhang, X.H.; Maeda, N.; Craig, V.S.J. Physical properties of nanobubbles on hydrophobic surfaces in water and aqueous solutions. *Langmuir* **2006**, *22*, 5025–5035. [CrossRef] [PubMed]

79. Nagayama, G.; Tsuruta, T.; Cheng, P. Molecular dynamics simulation on bubble formation in a nanochannel. *Int. J. Heat Mass Transf.* **2006**, *49*, 4437–4443. [CrossRef]

80. Ushikubo, F.Y.; Enari, M.; Furukawa, T.; Nakagawa, R.; Makino, Y.; Kawagoe, Y.; Oshita, S. Zeta-potential of micro-and/or nano-bubbles in water produced by some kinds of gases. *IFAC Proc. Vol.* **2010**, *43*, 283–288. [CrossRef]

81. Yasui, K.; Tuziuti, T.; Kanematsu, W.; Kato, K. Dynamic equilibrium model for a bulk nanobubble and a microbubble partly covered with hydrophobic material. *Langmuir* **2016**, *32*, 11101–11110. [CrossRef]

82. Yasui, K.; Tuziuti, T.; Kanematsu, W. High temperature and pressure inside a dissolving oxygen nanobubble. *Ultrason. Sonochemistry* **2019**, *55*, 308–312. [CrossRef]

83. Li, H.; Hu, L.; Song, D.; Al-Tabbaa, A. Subsurface transport behavior of micro-nano bubbles and potential applications for groundwater remediation. *Int. J. Environ. Res. Public Health* **2014**, *11*, 473–486. [CrossRef]

84. Hong, T.; Ye, C.; Li, C.H.; Zhang, B.J.; Zhou, L. Treatment effect of microbubble aeration technology on black-odor river water. *J. Environ. Eng. Technol.* **2011**, *1*, 20–25.

85. Temesgen, T. Enhancing Gas-Liquid Mass Transfer and (Bio) Chemical Reactivity Using Ultrafine/Nanobubble in Water and Waste Water Treatments. Ph.D. Thesis, Department of Civil and Environmental Engineering, Seoul National University, Seoul, Republic of Korea, 2017.

86. Zhang, M.; Qiu, L.; Liu, G. Basic characteristics and application of micro-nano bubbles in water treatment. *IOP Conf. Ser. Earth Environ. Sci.* **2020**, *510*, 042050. [CrossRef]

87. Ljunggren, S.; Eriksson, J.C. The lifetime of a colloid-sized gas bubble in water and the cause of the hydrophobic attraction. *Colloids Surf. A Physicochem. Eng. Asp.* **1997**, *129*, 151–155. [CrossRef]

88. Henry, W. Experiments on the quantity of gases absorbed by water, at different temperatures, and under different pressures. In *Abstracts of the Papers Printed in the Philosophical Transactions of the Royal Society of London*; The Royal Society: London, UK, 1832; pp. 103–104.

89. Shen, D.; Xie, Z.; Shentu, J.; Long, Y.; Lu, L.; Li, L.; Qi, S. Enhanced oxidation of aromatic hydrocarbons by ozone micro-nano bubble water: Mechanism and influencing factors. *J. Environ. Chem. Eng.* **2023**, *11*, 110281. [CrossRef]

90. Jin, N.; Zhang, F.; Cui, Y.; Sun, L.; Gao, H.; Pu, Z.; Yang, W. Environment-friendly surface cleaning using micro-nano bubbles. *Particuology* **2022**, *66*, 1–9. [CrossRef]

91. Takahashi, M.; Chiba, K.; Li, P. Free-radical generation from collapsing microbubbles in the absence of a dynamic stimulus. *J. Phys. Chem. B* **2007**, *111*, 1343–1347. [CrossRef] [PubMed]

92. Takahashi, M.; Ishikawa, H.; Asano, T.; Horibe, H. Effect of microbubbles on ozonized water for photoresist removal. *J. Phys. Chem. C* **2012**, *116*, 12578–12583. [CrossRef]

93. Kohno, M.; Mokudai, T.; Ozawa, T.; Niwano, Y. Free radical formation from sonolysis of water in the presence of different gases. *J. Clin. Biochem. Nutr.* **2011**, *49*, 96–101. [CrossRef]

94. Jia, W.; Ren, S.; Hu, B. Effect of water chemistry on zeta potential of air bubbles. *Int. J. Electrochem. Sci.* **2013**, *8*, 5828–5837. [CrossRef]

95. Takahashi, M. The ζ potential of microbubbles in aqueous solutions—Electrical properties of the gas-water interface. *J. Phys. Chem.* **2005**, *109*, 21858–21864. [CrossRef]

96. Ushikubo, F.Y.; Furukawa, T.; Nakagawa, R.; Enari, M.; Makino, Y.; Kawagoe, Y.; Shiina, T.; Oshita, S. Evidence of the existence and the stability of nano-bubbles in water. *Colloids Surf. A Physicochem. Eng. Asp.* **2010**, *361*, 31–37. [CrossRef]

97. Khaled Abdella Ahmed, A.; Sun, C.; Hua, L.; Zhang, Z.; Zhang, Y.; Marhaba, T.; Zhang, W. Colloidal properties of air, oxygen, and nitrogen nanobubbles in water: Effects of ionic strength, natural organic matters, and surfactants. *Environ. Eng. Sci.* **2018**, *35*, 720–727. [CrossRef]

98. Meegoda, J.N.; Aluthgun Hewage, S.; Batagoda, J.H. Stability of nanobubbles. *Environ. Eng. Sci.* **2018**, *35*, 1216–1227. [CrossRef]

99. Hamamoto, S.; Takemura, T.; Suzuki, K.; Nishimura, T. Effects of pH on nano-bubble stability and transport in saturated porous media. *J. Contam. Hydrol.* **2018**, *208*, 61–67. [CrossRef]

100. Li, H. Study on the Water, Fertilization and Aeration Distribution Characteristics of Aerated Drip Irrigation, and the Clogging of Emitters. Ph.D. Thesis, Jiangsu University, Zhenjiang, China, 2020.

101. Yan, C.C.; Cun, H.H.; Zhang, H.Y.; Chen, L.; Liu, Y.L. Numerical simulation of effects of microbubble growth and collapse on adjacent microspheres. *Chin. J. Appl. Mech.* **2022**, *36*, 580–587.

102. Kröninger, D.; Köhler, K.; Kurz, T.; Lauterborn, W. Particle tracking velocimetry of the flow field around a collapsing cavitation bubble. *Exp. Fluids* **2010**, *48*, 395–408. [CrossRef]

103. Zwaan, E.; Le Gac, S.; Tsuji, K.; Ohl, C.-D. Controlled cavitation in microfluidic systems. *Phys. Rev. Lett.* **2007**, *98*, 254501. [CrossRef]

104. Yasui, K.; Tuziuti, T.; Kanematsu, W. Extreme conditions in a dissolving air nanobubble. *Phys. Rev. E* **2016**, *94*, 013106. [CrossRef]

105. Yasui, K. Alternative model of single-bubble sonoluminescence. *Phys. Rev. E* **1997**, *56*, 6750. [CrossRef]

106. Yasui, K.; Tuziuti, T.; Sivakumar, M.; Iida, Y. Theoretical study of single-bubble sonochemistry. *J. Chem. Phys.* **2005**, *122*, 224706. [CrossRef] [PubMed]

107. Wang, B.; Su, H.; Zhang, B. Hydrodynamic cavitation as a promising route for wastewater treatment—A review. *Chem. Eng. J.* **2021**, *412*, 128685. [CrossRef]

108. Sun, X.; Park, J.J.; Kim, H.S.; Lee, S.H.; Seong, S.J.; Om, A.S.; Yoon, J.Y. Experimental investigation of the thermal and disinfection performances of a novel hydrodynamic cavitation reactor. *Ultrason. Sonochemistry* **2018**, *49*, 13–23. [CrossRef] [PubMed]

109. Khuntia, S.; Majumder, S.K.; Ghosh, P. Quantitative prediction of generation of hydroxyl radicals from ozone microbubbles. *Chem. Eng. Res. Des.* **2015**, *98*, 231–239. [CrossRef]

110. Yu, X.; Wang, Z.; Lv, Y.; Wang, S.; Zheng, S.; Du, H.; Zhang, Y. Effect of microbubble diameter, alkaline concentration and temperature on reactive oxygen species concentration. *J. Chem. Technol. Biotechnol.* **2017**, *92*, 1738–1745. [CrossRef]

111. Li, P.; Takahashi, M.; Chiba, K. Enhanced free-radical generation by shrinking microbubbles using a copper catalyst. *Chemosphere* **2009**, *77*, 1157–1160. [CrossRef] [PubMed]

112. Takahashi, M.; Chiba, K.; Li, P. Formation of hydroxyl radicals by collapsing ozone microbubbles under strongly acidic conditions. *J. Phys. Chem. B* **2007**, *111*, 11443–11446. [CrossRef] [PubMed]

113. Gottschalk, C.; Libra, J.A.; Saupe, A. *Ozonation of Water and Waste Water: A Practical Guide to Understanding Ozone and Its Applications*; John Wiley & Sons: Hoboken, NJ, USA, 2009.

114. Li, P.; Takahashi, M.; Chiba, K. Degradation of phenol by the collapse of microbubbles. *Chemosphere* **2009**, *75*, 1371–1375. [CrossRef]

115. Kondo, T.; Gamson, J.; Mitchell, J.B.; Riesz, P. Free radical formation and cell lysis induced by ultrasound in the presence of different rare gases. *Int. J. Radiat. Biol.* **1988**, *54*, 955–962. [CrossRef]

116. Fan, W.; Li, Y.; Lyu, T.; Yu, J.; Chen, Z.; Jarvis, P.; Huo, Y.; Xiao, D.; Huo, M. A modelling approach to explore the optimum bubble size for micro-nanobubble aeration. *Water Res.* **2023**, *228*, 119360. [CrossRef]

117. Wang, X.; Wang, J.; Guo, P.; Guo, W.; Li, G. Chemical effect of swirling jet-induced cavitation: Degradation of rhodamine B in aqueous solution. *Ultrason. Sonochemistry* **2008**, *15*, 357–363. [CrossRef] [PubMed]

118. Wang, X.; Zhang, Y. Degradation of alachlor in aqueous solution by using hydrodynamic cavitation. *J. Hazard. Mater.* **2009**, *161*, 202–207. [CrossRef] [PubMed]

119. Thompson, L.H.; Doraiswamy, L.K. Sonochemistry: Science and engineering. *Ind. Eng. Chem. Res.* **1999**, *38*, 1215–1249. [CrossRef]

120. Frontistis, Z.; Mantzavinos, D. Sonodegradation of 17α-ethynylestradiol in environmentally relevant matrices: Laboratory-scale kinetic studies. *Ultrason. Sonochemistry* **2012**, *19*, 77–84. [CrossRef] [PubMed]

121. Masuda, N.; Maruyama, A.; Eguchi, T.; Hirakawa, T.; Murakami, Y. Influence of microbubbles on free radical generation by ultrasound in aqueous solution: Dependence of ultrasound frequency. *J. Phys. Chem. B* **2015**, *119*, 12887–12893. [CrossRef] [PubMed]

122. Makuta, T.; Aizawa, Y.; Suzuki, R. Sonochemical reaction with microbubbles generated by hollow ultrasonic horn. *Ultrason. Sonochemistry* **2013**, *20*, 997–1001. [CrossRef] [PubMed]

123. Li, Y.J. Formation and Characterization of Bulk Micro-/Nanobubbles. Master's Thesis, Xi'an University of Architecture and Technology, Xi'an, China, 2020.

124. Tasaki, T.; Wada, T.; Fujimoto, K.; Kai, S.; Ohe, K.; Oshima, T.; Bada, Y.; Kukizaki, M. Degradation of methyl orange using short-wavelength UV irradiation with oxygen microbubbles. *J. Hazard. Mater.* **2009**, *162*, 1103–1110. [CrossRef] [PubMed]

125. Gao, Y.; Duan, Y.; Fan, W.; Guo, T.; Huo, M.; Yang, W.; Zhu, S.; An, W. Intensifying ozonation treatment of municipal secondary effluent using a combination of microbubbles and ultraviolet irradiation. *Environ. Sci. Pollut. Res.* **2019**, *26*, 21915–21924. [CrossRef]

126. Lu, J.; Huang, X.; Zhang, Z.; Pang, H.; Chen, K.; Xia, H.; Sui, Y.; Chen, R.; Zhao, Z. Co-coagulation of micro-nano bubbles (MNBs) for enhanced drinking water treatment: A study on the efficiency and mechanism of a novel cleaning process. *Water Res.* **2022**, *226*, 119245. [CrossRef]

127. Xia, Z.; Hu, L. Treatment of organics contaminated wastewater by ozone micro-nano-bubbles. *Water* **2018**, *11*, 55. [CrossRef]

128. Xia, Z.; Hu, L. Remediation of organics contaminated groundwater by ozone micro-nano bubble. *Jpn. Geotech. Soc. Spec. Publ.* **2016**, *2*, 1978–1981. [CrossRef]

129. Achar, J.C.; Nam, G.; Jung, J.; Klammler, H.; Mohamed, M.M. Microbubble ozonation of the antioxidant butylated hydroxytoluene: Degradation kinetics and toxicity reduction. *Environ. Res.* **2020**, *186*, 109496. [CrossRef] [PubMed]

130. Jabesa, A.; Ghosh, P. Removal of diethyl phthalate from water by ozone microbubbles in a pilot plant. *J. Environ. Manag.* **2016**, *180*, 476–484. [CrossRef] [PubMed]

131. Cheng, W.; Quan, X.; Li, R.; Wu, J.; Zhao, Q. Ozonation of phenol-containing wastewater using $O_3/Ca(OH)_2$ system in a micro bubble gas-liquid reactor. *Ozone Sci. Eng.* **2018**, *40*, 173–182. [CrossRef]

132. Li, P.; Tsuge, H.; Itoh, K. Oxidation of dimethyl sulfoxide in aqueous solution using microbubbles. *Ind. Eng. Chem. Res.* **2009**, *48*, 8048–8053. [CrossRef]

133. Teo, K.C.; Xu, Y.; Yang, C. Sonochemical degradation for toxic halogenated organic compounds. *Ultrason. Sonochemistry* **2001**, *8*, 241–246. [CrossRef]

134. Kalumuck, K.M.; Chahine, G.L. The use of cavitating jets to oxidize organic compounds in water. *J. Fluids Eng.* **2000**, *122*, 465–470. [CrossRef]

135. Xia, Z.; Hu, L.; Kusaba, S.; Song, D. Remediation of TCE contaminated site by ozone micro-nano-bubbles. In *The International Congress on Environmental Geotechnics*; Springer: Singapore, 2018; pp. 796–803.

136. Kim, I.K.; Huang, C.P. Sonochemical degradation of polycyclic aromatic sulfur hydrocarbons (PASHs) in aqueous solutions exemplified by benzothiophene. *J. Chin. Inst. Eng.* **2005**, *28*, 1107–1118. [CrossRef]

137. Hu, Y.Y.; Zhu, K.Q.; Xi, B.S. Numercial study of cavitation erosion on a rigid wall. *Chin. J. Appl. Mech.* **2004**, *21*, 22–25.

138. Lakretz, A.; Ron, E.Z.; Mamane, H. Biofilm control in water by a UV-based advanced oxidation process. *Biofouling* **2011**, *27*, 295–307. [CrossRef]

139. Gogate, P.R.; Kabadi, A.M. A review of applications of cavitation in biochemical engineering/biotechnology. *Biochem. Eng. J.* **2009**, *44*, 60–72. [CrossRef]

140. Shirgaonkar, I.Z.; Lothe, R.R.; Pandit, A.B. Comments on the mechanism of microbial cell disruption in high-pressure and high-speed devices. *Biotechnol. Prog.* **1998**, *14*, 657–660. [CrossRef] [PubMed]

141. Mason, T.; Joyce, E.; Phull, S.; Lorimer, J. Potential uses of ultrasound in the biological decontamination of water. *Ultrason. Sonochemistry* **2003**, *10*, 319–323. [CrossRef] [PubMed]

142. Tan, S.Y.; Shen, Y.; Liu, Y.Z.; Wang, X.; Xiao, Y.; Li, Y. Effects and mechanism of using Nanobubble to inhibit biofouling and scaling in biogas slurry drip irrigation emitters. *Trans. Chin. Soc. Agric. Eng.* **2022**, *38*, 79–87.

143. Wang, X.Y. Mechanism and Application Research of the Emitters Clogging Control Method by Micro-Nano Bubbles of Drip Irrigation Systems with Biogas Slurry. Master's Thesis, Shihezi University, Shihezi, China, 2020.

144. Agarwal, A.; Ng, W.J.; Liu, Y. Cleaning of biologically fouled membranes with self-collapsing microbubbles. *Biofouling* **2013**, *29*, 69–76. [CrossRef] [PubMed]

145. Khadre, M.A.; Yousef, A.E.; Kim, J.G. Microbiological aspects of ozone applications in food: A review. *J. Food Sci.* **2001**, *66*, 1242–1252. [CrossRef]

146. Zhu, Z.; Shan, L.; Li, X.; Hu, F.; Yuan, Y.; Zhong, D.; Zhang, J. Effects of interspecific interactions on biofilm formation potential and chlorine resistance: Evaluation of dual-species biofilm observed in drinking water distribution systems. *J. Water Process. Eng.* **2020**, *38*, 101564. [CrossRef]

147. Bimakr, F.; Ginige, M.P.; Kaksonen, A.H.; Sutton, D.C.; Puzon, G.J.; Cheng, K.Y. Assessing graphite and stainless-steel for electrochemical sensing of biofilm growth in chlorinated drinking water systems. *Sens. Actuators B Chem.* **2018**, *277*, 526–534. [CrossRef]

148. McEwan, C.; Kamila, S.; Owen, J.; Nesbitt, H.; Callan, B.; Borden, M.; Nomikou, N.; Hamoudi, R.A.; Taylor, M.A.; Stride, E.; et al. Combined sonodynamic and antimetabolite therapy for the improved treatment of pancreatic cancer using oxygen loaded microbubbles as a delivery vehicle. *Biomaterials* **2016**, *80*, 20–32. [CrossRef]

149. McEwan, C.; Owen, J.; Stride, E.; Fowley, C.; Nesbitt, H.; Cochrane, D.; Coussios, C.; Borden, M.; Nomikou, N.; McHale, A.P.; et al. Oxygen carrying microbubbles for enhanced sonodynamic therapy of hypoxic tumours. *J. Control. Release* **2015**, *203*, 51–56. [CrossRef]